Age, chemistry, and tectonic setting of Miramichi terrane (Early Paleozoic) volcanic rocks, eastern and east-central Maine, USA

Allan Ludman[1,*], Christopher McFarlane[2], and Amber T. H. Whittaker[3]

1. School of Earth and Environmental Sciences, Queens College (CUNY), Flushing, New York 11367, USA
and CUNY Graduate Center, New York, New York
2. Department of Earth Sciences, University of New Brunswick, Fredericton, New Brunswick E3B 5A3, Canada
3. Maine Geological Survey, 93 State House Station, 17 Elkins Lane, Augusta, Maine 04433, USA
*Corresponding author <allan.ludman@qc.cuny.edu>

ABSTRACT

Volcanic rocks in the Miramichi inlier in Maine occur in two areas separated by the Bottle Lake plutonic complex: the Danforth segment (Stetson Mountain Formation) north of the complex and Greenfield segment to the south (Olamon Stream Formation). Both suites are dominantly pyroclastic, with abundant andesite, dacite, and rhyolite tuffs and subordinate lavas, breccias, and agglomerates. Rare basaltic tuffs and a small area of basaltic tuffs, agglomerates, and lavas are restricted to the Greenfield segment. U–Pb zircon geochronology dates Greenfield segment volcanism at ca. 469 Ma, the Floian–Dapingian boundary between the Lower and Middle Ordovician. Chemical analyses reveal a calc-alkaline suite erupted in a continental volcanic arc, either the Meductic or earliest Balmoral phase of Popelogan arc activity.

The Maine Miramichi volcanic rocks are most likely correlative with the Meductic Group volcanic suite in west-central New Brunswick. Orogen-parallel lithologic and chemical variations from New Brunswick to east-central Maine may result from eruptions at different volcanic centers. The bimodal Poplar Mountain volcanic suite at the Maine–New Brunswick border is 10–20 myr younger than the Miramichi volcanic rocks and more likely an early phase of back-arc basin rifting than a late-stage Meductic phase event. Coeval calc-alkaline arc volcanism in the Miramichi, Weeksboro–Lunksoos Lake, and Munsungun Cambrian–Ordovician inliers in Maine is not consistent with tectonic models involving northwestward migration of arc volcanism. This >150 km span cannot be explained by a single east-facing subduction zone, suggesting more than one subduction zone/arc complex in the region.

RÉSUMÉ

Les roches volcaniques de la boutonnière de Miramichi au Maine sont présentes dans deux secteurs séparés par le complexe plutonique du lac Bottle : le segment Danforth (Formation de Stetson Mountain) au nord du complexe et le segment Greenfield au sud (Formation d'Olamon Stream). Les deux séquences sont constituées en prédominance de roches pyroclastiques, accompagnées d'une abondance de tufs andésitiques, dacitiques et rhyolitiques ainsi que de laves, de brèches et d'agglomérats subordonnés. De rares tufs basaltiques et un petit secteur de tufs basaltiques, d'agglomérats et de laves se restreignent au segment Greenfield. Une datation U–Pb sur zircon situe le volcanisme du segment Greenfield à environ 469 Ma, c'est-à-dire la limite du Floien-Dapingien, entre l'Ordovicien inférieur et moyen. Des analyses chimiques révèlent qu'une séquence calco-alcaline est entrée en éruption dans un arc volcanique continental, soit la phase de Meductic, soit la phase la plus précoce de Balmoral de la manifestation de l'arc de Popelogan.

Les roches volcaniques de Miramichi au Maine sont très probablement corrélatives de la séquence volcanique du groupe de Meductic dans le centre-ouest du Nouveau-Brunswick. Les variations lithologiques et chimiques parallèles à l'orogène du Nouveau-Brunswick au centre-est du Maine pourraient découler d'éruptions de différents centres volcaniques. La séquence volcanique bimodale du mont Poplar sur la frontière entre le Maine et le Nouveau-Brunswick est plus récente de 10 à 20 Ma que les roches volcaniques de Miramichi et elle représente plus vraisemblablement une phase précoce de la distension d'un bassin arrière-arc qu'un phénomène de stade tardif de la phase de Meductic. Le volcanisme d'arc contemporain dans les boutonnières cambro-ordoviciennes de Miramichi, de Weeksboro–lac Lunksoos et de Munsungun au Maine ne correspond pas aux modèles tectoniques de migration vers le nord-ouest du volcanisme d'arc. Cet intervalle de plus de 150 kilomètres ne peut pas être expliqué par une seule zone de subduction orientée vers l'est, ce qui laisse supposer plus d'une zone de subduction/ d'un complexe d'arc dans la région.

[*Traduit par la redaction*]

INTRODUCTION

The Early Paleozoic tectonic evolution of the northern Appalachian orogen in Maine and New Brunswick is recorded in northeast-trending inliers of Late Cambrian to Middle Ordovician strata, separated today by broad bands of Late Ordovician to Early Devonian cover rocks (Fig. 1). The Miramichi terrane is the largest of these inliers, extending more than 250 km from Bathurst in northern New Brunswick to the Danforth area at the New Brunswick/Maine border, after which it narrows rapidly and terminates about 100 km farther to the southwest, south of Greenfield (see Ludman 2020).

The youngest strata throughout the Miramichi terrane are thick sections of volcanic rock, most intensely studied in the Bathurst area where they host volcanogenic sulfide deposits (van Staal *et al.* 2003). The ages and chemistry of Miramichi volcanic rocks in New Brunswick reveal the timing of arc-related volcanism associated with the accretion of the Ganderian plate to ancestral North America (Winchester *et al.* 1992; Fyffe 2001; van Staal *et al.* 2016), but little information has been available about volcanic rocks in the Maine segment, making it impossible to investigate similarities or differences along the length of the terrane. This paper presents new and previously unpublished data on the chemical compositions and ages of Miramichi volcanic rocks in Maine that permit a more comprehensive view of Miramichi volcanism, its roles in Ganderian accretion, and its relationships to other pre-Silurian belts.

Tectonic setting

The Paleozoic evolution of the Appalachian orogen in New England and adjacent Atlantic Canada involved the progressive accretion to ancestral North America (Laurentia) of the outboard Gander, Avalon, and Meguma peri-Gondwanan plates (Fig. 2a), resulting in the current lithotectonic framework (Fig. 2b). Ganderia is the largest accreted plate (Fig. 2b), and studies of Ganderian volcanic units in the northern Miramichi, Elmtree, and Popelogan inliers in New Brunswick have yielded a detailed picture of subduction and associated opening and closing of back-arc basins in the central part of the plate (Table 1; van Staal *et al.* 2016). Previous tectonic models have focused on the nature and sequence

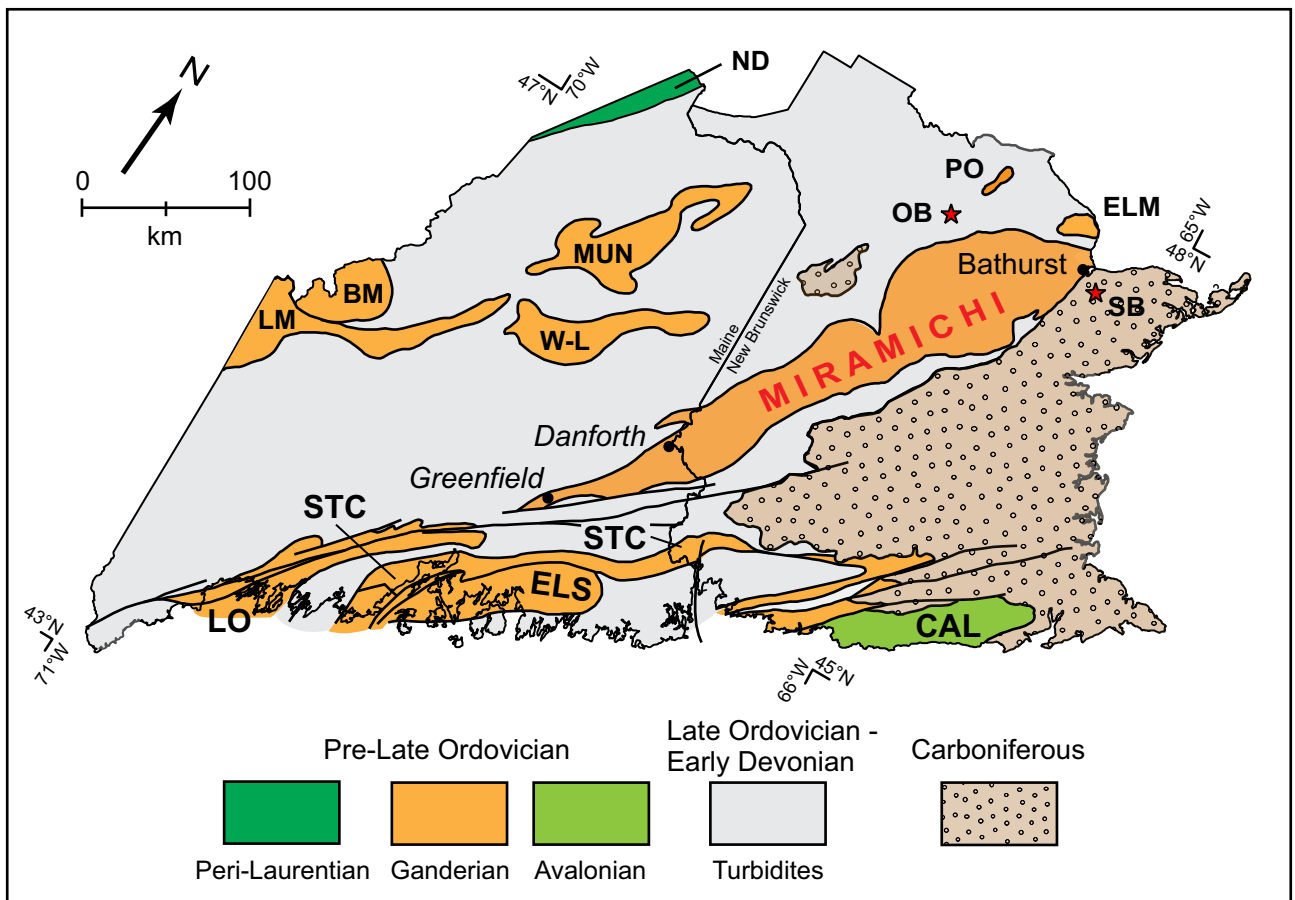**Figure 1.** Simplified map showing the Miramichi terrane and other Cambrian–Ordovician inliers and younger cover rocks in Maine and New Brunswick. BM = Boundary Mountain; CAL = Caledonia; ELM = Elmtree; ELS = Ellsworth; LM = Lobster Mountain; LO = Liberty–Orrington; MUN = Munsungun; ND = Notre Dame; OB = Oxford Brook; PO = Popelogan; SB = Straughan Brook; STC = St. Croix; WL = Weeksboro–Lunksoos.
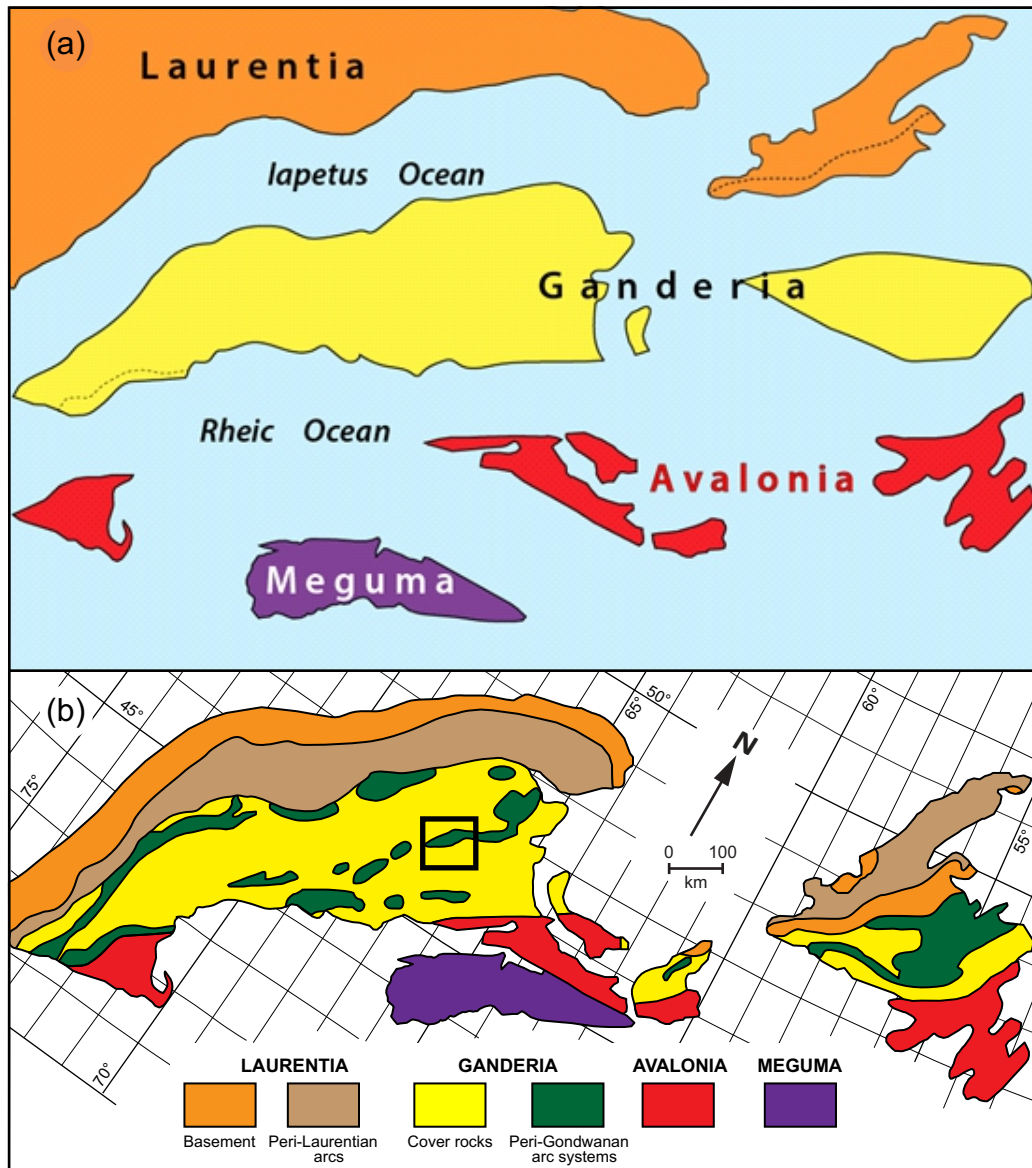
Figure 2. Schematic relationships of the Laurentian plate and peri-Gondwanan plate fragments in the northern Appalachians. **(a)** Cambrian (not to scale). **(b)** Current. Rectangle outlines study area in eastern and east-central Maine (after Hibbard *et al.* 2006).

of plate accretion events. This paper complements and helps evaluate those models, but also makes possible comparison of volcanism along the length of the Miramichi inlier.

Geologic setting

Figure 3 shows relationships of the Miramichi terrane with younger cover rocks of the Central Maine/Aroostook–Matapedia (CMAM) basin to the northwest and the Fredericton trough to the southeast. The Miramichi study area shown in Figure 3 has experienced only lower greenschist facies regional metamorphism (chlorite and sub-chlorite zones) and thus represents a supracrustal level of the northern Appalachians (Ludman 2020). Delicate primary features are generally well preserved, including shard outlines in Mi-

ramichi volcanic rocks described below.

The Miramichi terrane in Maine is divided into two segments by the ca. 380 Ma Bottle Lake plutonic complex: the Danforth segment between the complex and the New Brunswick border, and the smaller Greenfield segment southwest of the complex (Fig. 3). The Pokiok igneous complex at the Maine–New Brunswick border further separates the Maine part of the inlier from the southwestern New Brunswick components.

Regional-scale faults separate the Miramichi terrane from adjacent cover rocks. The southeastern contact with the Fredericton trough is the Codyville fault in the Danforth segment, northwesternmost branch of the transcurrent Norumbega fault system, and the Southeast Boundary Fault, its possible continuation, in the Greenfield segment. The evolution

Table 1. Tectonic timeline relationships of the Laurentian plate and peri-Gondwanan plate fragments.

	AGE	OROGENY	TECTONIC EVENTS
APPALACHIAN WILSON CYCLE	Permian	Alleghanian	Gondwana accreted to previously amalgamated plates forming supercontinent Pangea
	Late Devonian	"Neoacadian"	Meguma accreted to previously amalgamated plates
	Early Devonian	Acadian	Avalon accreted to previously amalgamated plates
	Late Silurian	Salinic	Accretion of Ganderia to Laurentia completed by closure of remnant back-arc basin at trailing edge of Ganderia
	Silurian	Early Salinic	Continued Ganderia-Laurentia convergence by closure of Tetagouche back-arc basin (Miramichi inlier)
	Late Ordovician	"Taconic"	Leading edge of Ganderia collides with Laurentia
	Ordovician		Continued Ganderia-Laurentia convergence
	Cambrian–Ordovician	Penobscot	Ganderian components (Miramichi, Annidale,) reunited near trailing edge of the Ganderian plate
	Cambrian–Early Ordovician		Ganderia rifted from Gondwana, drifts toward Laurentia, and is fragmented by extension during Iapetan subduction that produces island arcs and back-arc basins
	Latest Neoproterozoic		Rifting of Rodinia, opening of Iapetus Ocean
	Neoproterozoic (~1Ga)	Grenville	Assembly of supercontinent Rodinia

of the western contact was complex, with the Northwest Boundary, Stetson Mountain, and North Bancroft faults locally separating Miramichi from CMAM strata. Evolution of these boundaries and their relationships with faults in New Brunswick is beyond the scope of this paper; for details see Ludman (in press).

Previous studies of Miramichi volcanic rocks in Maine

Despite its tectonic significance, the Miramichi terrane in Maine received little attention from previous investigators. The first modern report was a United States Geological Survey regional reconnaissance study of central eastern Maine that included the Danforth segment but did not extend as far southwest as the Greenfield area (Larrabee *et al.* 1965). That study briefly described volcanic rocks to which a Middle to Late Ordovician age was assigned based on graptolites in a black shale horizon just north of Danforth. It also suggested similarities with the Tetagouche volcanic section in northern New Brunswick and with rocks of the Weeksboro–Lunksoos Lake belt in northern Maine. Detailed mapping between 1980 and 2020 established and refined Danforth segment stratigraphy and interpreted a complex, multideformation tectonic history described below (Ludman 1985, 1991, 2003, 2020; Ludman and Berry 2003; Ludman and Hopeck 2020).

Sayres (1986) suggested an internal stratigraphy for Miramichi volcanic rocks in the Danforth 15′ quadrangle (see

below) and reported chemical analyses revealing a calc-alkaline suite of andesite, rhyodacite, and rhyolite that she interpreted as a volcanic arc assemblage (Sayres 1986). A study of the Meductic arc in southwestern New Brunswick included a few samples from the Danforth area, and supported Sayres' tectonic interpretation (Winchester *et al.* 1992).

The Greenfield segment was first studied by Olson (1972) in the southwestern part of what is now the Greenfield 7½′ quadrangle. His Masters thesis described a thick volcanic section composed mostly of andesitic and rhyolitic pyroclastic rocks but provided no chemical data. He tentatively correlated the volcanic rocks with those in the Danforth area and with the Weeksboro–Lunksoos Lake section based on descriptions in Larrabee *et al.* (1965) and Neuman (1962), respectively. Greenfield segment stratigraphy has been revised and volcanic geochemistry reported in recent studies of the Greenfield 7½′ quadrangle (Ludman 2020, in press).

Stratigraphy of the Miramichi terrane in Maine

A well-defined stratigraphy in the Danforth segment is truncated by the Bottle Lake pluton, but its basal Baskahegan Lake and Bowers Mountain formations reappear at the northern margin of the Greenfield segment (Fig. 4). The Bowers Mountain is absent in the southern part of the Greenfield segment, where a unique, thin-bedded Lazy
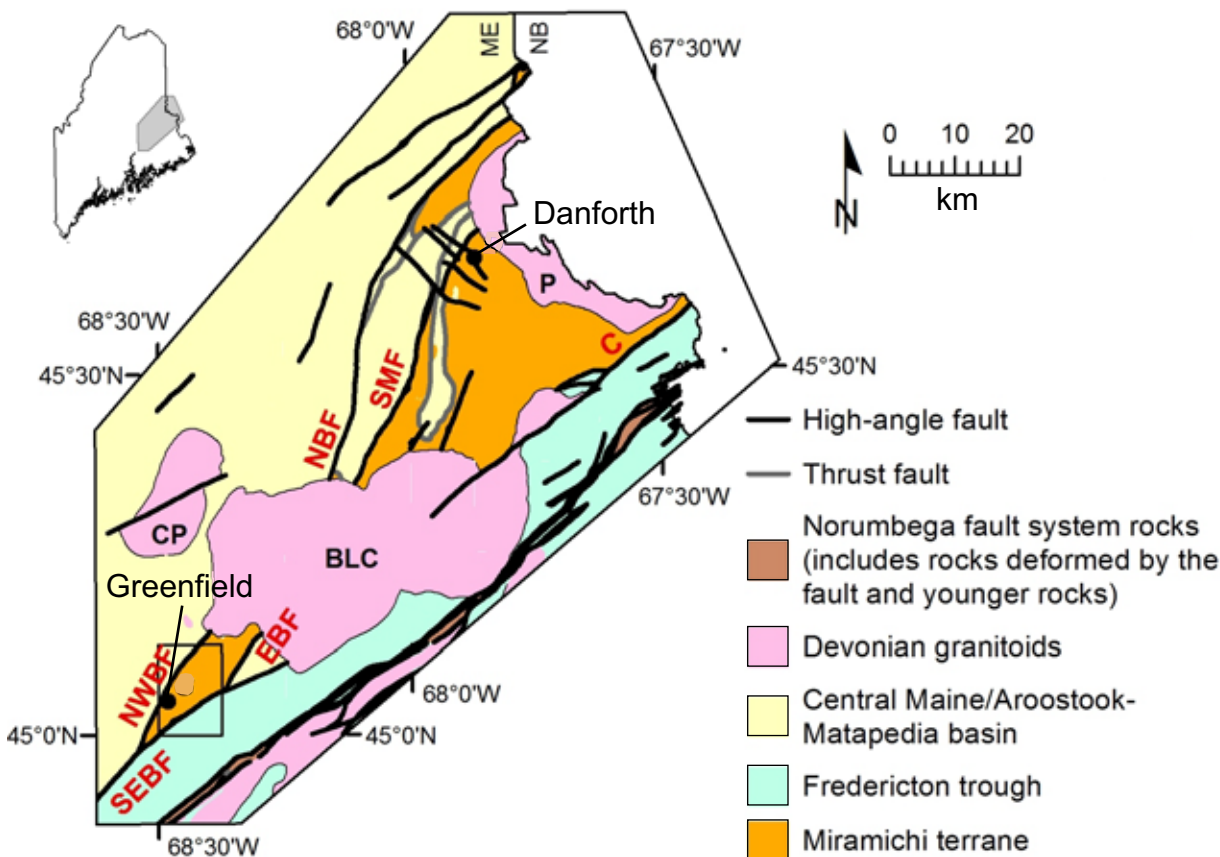
LUDMAN ET AL. – Age, chemistry, and tectonic setting of Miramichi terrane (Early Paleozoic) volcanic rocks, eastern and east-central Maine, USA

Copyright © Atlantic Geology, 2021

Figure 3. Simplified geologic map showing relationships of the Miramichi terrane with adjacent cover rocks after Ludman and Berry (2003), Ludman (2020), and unpublished mapping as of August 2020. Plutons: P = Pokiok; BLC = Bottle Lake igneous complex; CP = Center Pond. Faults: NWBF = Northwest Boundary Fault; SEBF = Southeast Boundary Fault; EBF = East Boundary fault; NBF = North Bancroft Fault; SMF = Stetson Mountain; C = Codyville strand of the Norumbega fault system.

Ledges Road member of the Baskahegan Lake Formation passes upward into volcanic rocks of the Olamon Stream Formation.

Thick volcanic suites cap the Miramichi section in both segments and, although similar, are different enough to require separate names – the Stetson Mountain Formation in the Danforth segment, and the Olamon Stream Formation in the Greenfield area. The Olamon Stream interpretation presented here is a revision of a recent report (Ludman 2020).

Sayres (1986) divided the Stetson Mountain Formation into a thin basal member of cryptocrystalline to fine grained felsic and intermediate ashfall tuff and a much thicker upper member of coarser felsic and intermediate ashflow tuff and agglomerate, separated by a thin, medial member of chalky weathering, black sooty iron- and manganese-rich volcanogenic (?) mudstone. A similar sequence appears to occur in the Olamon Stream Formation although outcrop control of the lower member is very poor. The lower member comprises mostly cryptocrystalline tuff, separated by an anoxic mudstone/siltstone (Greenfield member) from the upper member which appears to contain more abundant coarser pyroclastic rocks. The most significant difference between the two segments is the presence of relatively coarse grained

mafic volcanic (and subvolcanic?) rocks in the Greenfield segment. Unfortunately, the stratigraphic position of the mafic rocks within the Olamon Stream Formation is unknown.

MIRAMICHI VOLCANIC ROCKS IN MAINE

Rock types

The Danforth and Greenfield suites contain predominantly (>95%) pyroclastic rocks, a variety of intermingled intermediate (andesite, basaltic andesite) and felsic (dacite, rhyodacite, rhyolite) crystal, lithic, and crystal-lithic ashfall and ashflow tuffs, breccias, coarse agglomerates and subordinate lavas with rare volcaniclastic sedimentary horizons. Mafic rocks are largely confined to a small area at the southwest terminus of the Miramichi terrane, with sparse basaltic tuffs elsewhere in the Olamon Stream Formation. The most mafic rock in the Danforth segment is a low-silica basaltic andesite that occurs only as xenoliths in the Bottle Lake pluton and in a small fault-bounded sliver between that pluton and the Baskahegan Lake Formation.

Ludman et al. – Age, chemistry, and tectonic setting of Miramichi terrane (Early Paleozoic) volcanic rocks, eastern and east-central Maine, USA

Copyright © Atlantic Geology, 2021

Figure 4. Miramichi stratigraphy in Maine. Orange diamond = U–Pb zircon age. Formations: OЄbl = Baskahegan Lake; OЄbll = Lazy Ledges Road member; Obm = Bowers Mountain; Osm = Stetson Mountain; Oos = Olamon Stream (u, l, g = upper, lower, Greenfield members).

LUDMAN ET AL. – Age, chemistry, and tectonic setting of Miramichi terrane (Early Paleozoic) volcanic rocks, eastern and east-central Maine, USA

Copyright © Atlantic Geology, 2021

Felsic and intermediate rocks

Volcanic rocks of the Olamon Stream and Stetson Mountain formations are divided into three lithofacies that will be described in order of their abundance: ashfall tuffs; ashflow tuffs, breccias, and agglomerates and lavas.

Ashfall tuffs: Cryptocrystalline, almost porcelaneous felsic and intermediate tuffs make up the lower member of the Stetson Mountain Formation and about half of the Olamon Stream Formation (*aphanite* in Olson 1972). Most have been devitrified and sericitized, and the presence of microphenocrysts and/or small lithic fragments distinguish crystal, lithic, and crystal-lithic varieties. Cryptocrystalline tuffs that occur in homogeneous, featureless layers and lack evidence of flow are interpreted as ashfall deposits formed during Plinian eruptions. They are light to medium grey on fresh surfaces but weather to chalky white (Fig. 5) and typically fracture conchoidally. Layers deposited during individual eruptive events range widely in thickness from a few centimetres (Fig. 6a) to at least two metres (Fig. 6b) but style and thickness commonly vary within as well as between outcrops (Fig. 6c).

Microporphyritic variants are common, with some phenocrysts barely detectable with a hand lens. Quartz and feldspar microphenocrysts (0.2–0.5 mm) occur in rhyolites and rhyodacites, along with plagioclase and pyroxene (up to 2.5 mm) in andesites. Some small lithic fragments are also present.

Textural variations within layers formed in single eruptive events reflect changes in flow regime (Fig. 7). The most common variation is in grain size, with systematic changes (Figs. 7a, b) or fluctuations (Fig. 7c). In most cases, the changes are not useful as facing indicators, unless paired with geopetal indicators like the load cast in Figure 7c. In rare instances, the upper part of eruptive units is scoriaceous (Fig. 7d).

Ashflow tuffs, volcanic breccias, agglomerates, and lavas: Most felsic and intermediate volcanic rocks in the Danforth segment (Sayres 1986) and approximately 40% in the Greenfield segment are volcanic breccias (Fig. 8a) and agglomerates

Figure 6. Varied layering in felsic and intermediate tuffs. (a) Thin eruptive units. (b) Massive layers. (c) Pavement outcrop showing thin ashfall layers sandwiched between layers approximately 1 m thick.

Figure 5. Homogeneous cryptocrystalline ashfall tuff showing featureless fresh (left) and weathered (right) textures.

LUDMAN ET AL. – Age, chemistry, and tectonic setting of Miramichi terrane (Early Paleozoic) volcanic rocks, eastern and east-central Maine, USA
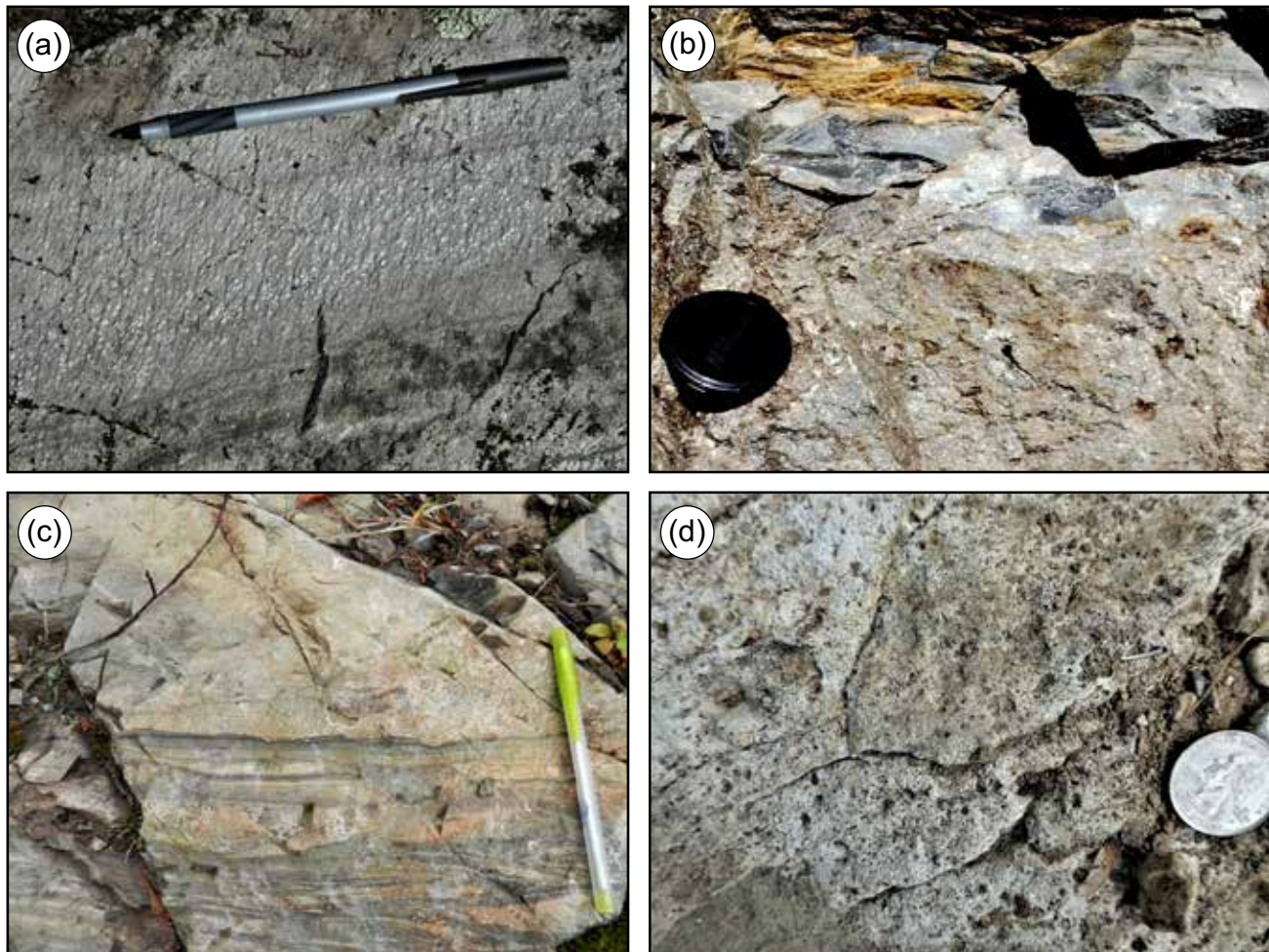
Copyright © Atlantic Geology, 2021

Figure 7. Variety of individual eruptive units. (a) Phenocrysts in layer beginning below the pen are absent from the lower part of the layer. (b) Cryptocrystalline (top) part of the layer transitions into porphyritic zone toward the bottom of the photograph. (c) Porphyritic basal part of eruptive unit (immediately above the load cast) becomes finer upward and coarsens again at the top. (d) scoriaceous top of flow.

with endogenous and exotic fragments (10 cm to 1 m in size) (Fig. 8b). Rare, imbricated fragments and foliation in coarse-grained and porphyritic lithic, crystal, or lithic-crystal tuffs (Fig. 8c) suggest eruption as ash and debris flows. Lava flows with microscopic to visible phenocrysts (Fig. 8d) are less common but are found throughout the volcanic suites in both segments.

Photomicrographs in Figure 9 illustrate the variety of felsic and intermediate textures. Matrix differences visible in thin section distinguish felsic and intermediate rocks and lava flows from tuffs. The matrix of most of the pyroclastic rocks has devitrified to a sericitized cryptocrystalline mosaic composed of quartz, feldspar, and rare chlorite in rhyolites and dacites (Fig. 9a, b), with less quartz and more abundant coarse patches of chlorite in andesites. Despite devitrification and sericitization, shard outlines are preserved in a few samples (Fig. 9c). Rocks with an interlocking matrix of feldspar ± quartz crystals are interpreted as lava flows. In most instances they have phenocrysts readily visible to the naked eye (Fig. 9e, f).

Feldspar microphenocrysts in rhyolitic tuffs are typically subhedral to euhedral whereas quartz occurs as subhedral to anhedral grains partly resorbed by the matrix mosaic. Plagioclase phenocrysts in rhyolite and rhyodacite are generally only slightly altered, but in andesites are heavily sericitized and may contain abundant carbonate, particularly in their cores. Hornblende phenocrysts in andesites are typically subhedral and twinned (Fig. 9f) and have been altered to chlorite ± epidote in some thin sections.

Sedimentary rocks: Horizons and individual beds of sedimentary rock make up a small percentage of the Olamon Stream and Stetson Mountain formations. Most are volcanogenic sandstone and coarse siltstone with subordinate grey pelite that can be difficult to recognize in the field because, like the volcanic rocks with which they are associated, they typically occur in thick, massive beds, weather chalky white and have a greenish cast caused by abundant detrital chlorite (Figs. 10a, b). They are distinguished in thin section by their detrital matrix rather than the interlocking or chloritized

LUDMAN ET AL. – Age, chemistry, and tectonic setting of Miramichi terrane
(Early Paleozoic) volcanic rocks, eastern and east-central Maine, USA
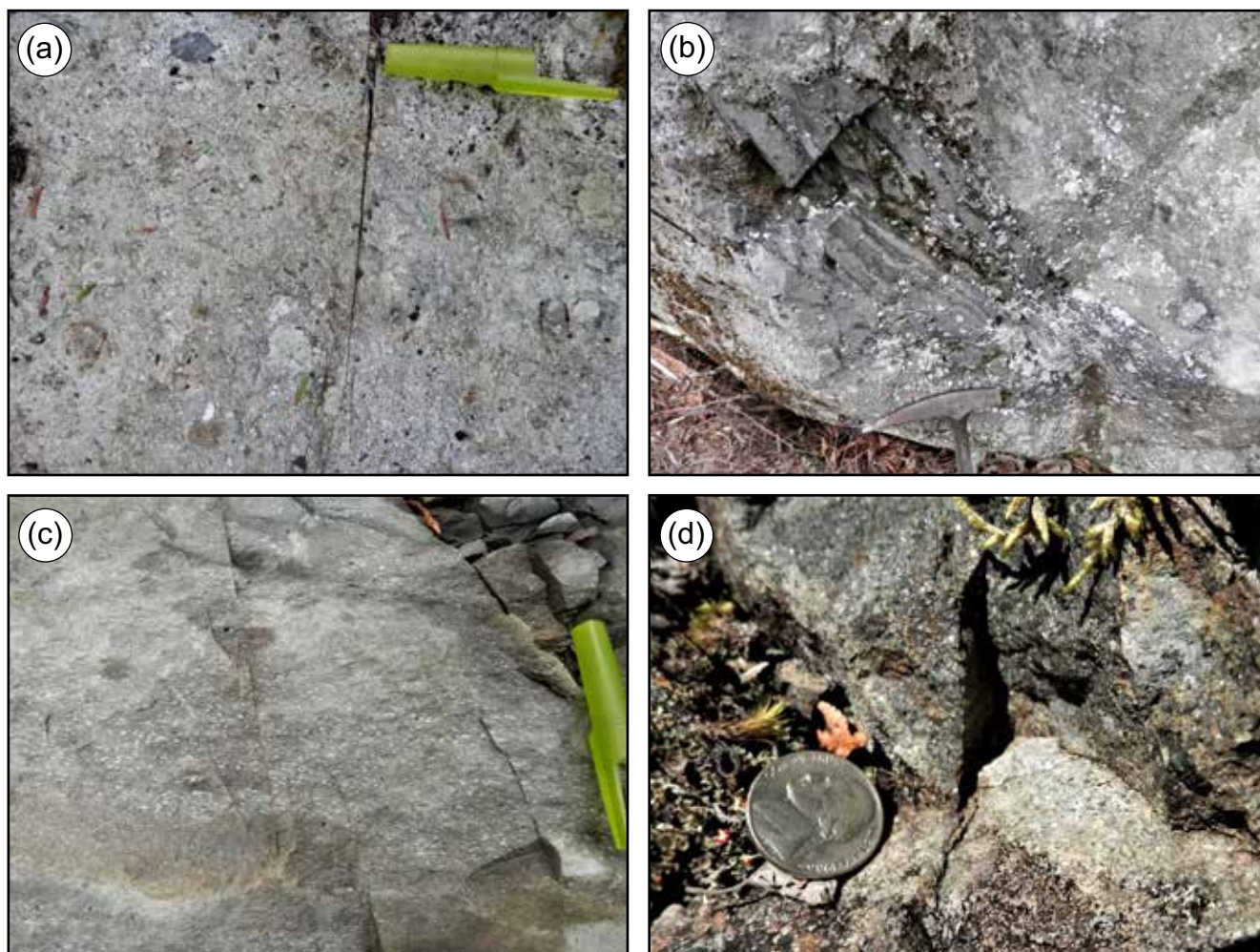
Copyright © Atlantic Geology, 2021

Figure 8. Textures of coarse-grained volcanic rocks. (a) Volcanic breccia. (b) Agglomerate with a large endogenous fragment. (c) Weakly foliated crystal tuff. (d) Unusually coarse rhyodacite lava with quartz and feldspar phenocrysts in an interlocking crystalline matrix (see Fig. 9e).

volcanic matrix of the pyroclastic rocks and lavas. Lenses and individual beds of black shale occur throughout the Olamon Stream and Stetson Mountain formations (Fig. 10c), and a unique horizon of maroon sandstone, siltstone, and shale crops out in the Greenfield quadrangle (Fig. 10d).

Mafic rocks

Basaltic lavas, ashflow tuffs, and volcanic agglomerates are minor constituents of the Greenfield segment and are mapped as a separate member of the Olamon Stream Formation (Ludman 2020, in press). Most are concentrated at the southwesternmost part of the Miramichi terrane just south of the Greenfield quadrangle, at the confluence of the Northwest and Southeast boundary faults. The contact between the mafic member and the main body of the Olamon Stream Formation is not exposed and their age relationships are unknown.

Basaltic tuffs also occur as individual layers within the Olamon Stream Formation, interbedded with andesite and dacite, but it is difficult to estimate their abundance because they are the same color (medium grey fresh surface, light grey to white weathered surfaces) and have the same fine to very fine-grained texture as the other rocks. Indeed, their presence was not suspected in the field and was revealed only by chemical analysis.

Two types of mafic rocks occur in the isolated terrane termination area, in roughly equal amounts – dark grey to greenish-grey, medium-grained basalt and greenstone, and coarse volcanic agglomerate. The former has seriate or porphyritic texture (Fig. 11a, b, c) and most occur in massive, nubbly weathering, featureless outcrops in which it is difficult to identify primary layering. Matrix and pyroxene phenocrysts are typically less altered than plagioclase in some (Fig. 11a) but highly chloritized in others (Fig. 11b). These rocks are interpreted as lavas but in the absence of primary layering, may be subvolcanic intrusions.

About half are agglomerate with clasts up to 40 cm set in a green, fine-grained, chlorite-rich, matrix. Most agglomerate exposures are massive, but a primary flow foliation has been
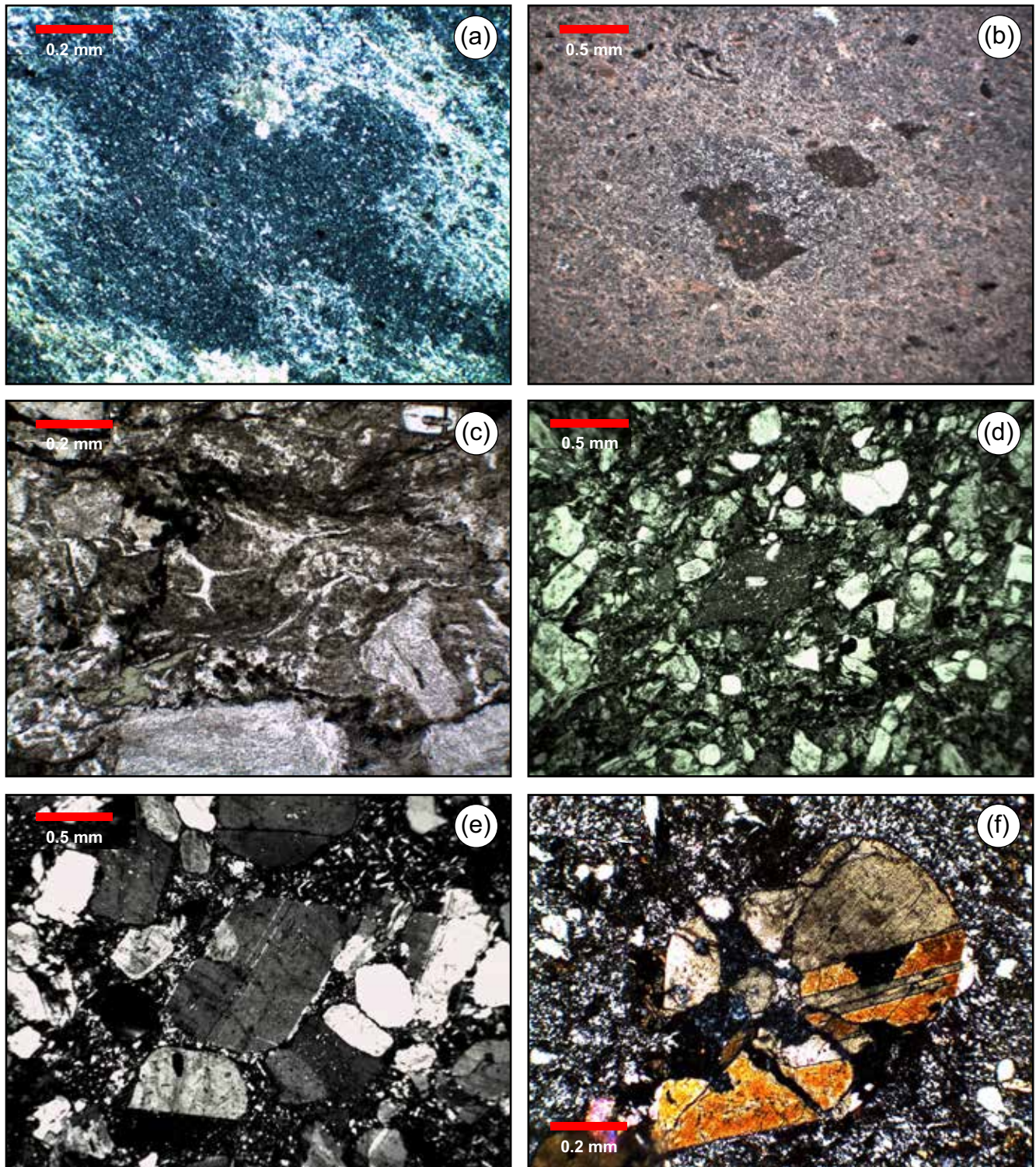
Figure 9. Photomicrographs showing textures of felsic and intermediate rocks. (a) Sericitized cryptocrystalline rhyolitic (ashfall) crystal tuff with quartz microphenocrysts, viewed under crossed polars. (b) Sericitized cryptocrystalline rhyolitic (ashfall) lithic-crystal tuff, viewed under crossed polars. (c) Coarser tuff with shards, quartz, and saussuritized feldspar phenocrysts with matrix chlorite patches, viewed in plane-polarized light. (d) Coarser tuff with quartz (partly resorbed) and feldspar phenocrysts with lithic fragments, viewed in plane-polarized light. (e) Rhyodacite lava displaying interlocking crystalline matrix with quartz and feldspar phenocrysts, viewed under crossed polars. (f) Andesite lava displaying interlocking crystalline matrix with twinned hornblende phenocryst, viewed under crossed polars.

Ludman et al. – Age, chemistry, and tectonic setting of Miramichi terrane
(Early Paleozoic) volcanic rocks, eastern and east-central Maine, USA

Copyright © Atlantic Geology, 2021

Figure 10. Olamon Stream Formation sedimentary rocks. **(a, b)** Volcaniclastic sandstone, siltstone, and shale. **(c)** Sulfidic black shale interbedded with tuff. **(d)** Maroon sandstone and siltstone.

observed locally. A few agglomerates contain only endogenous fragments (Fig. 11d) and are possibly autobreccias, but most contain both endogenous and exotic fragments – most commonly andesite or more felsic volcanic rock (Fig. 11e). A unique outcrop contains a mixture of mafic ashflow tuff, dark red baked mudstone, and large, 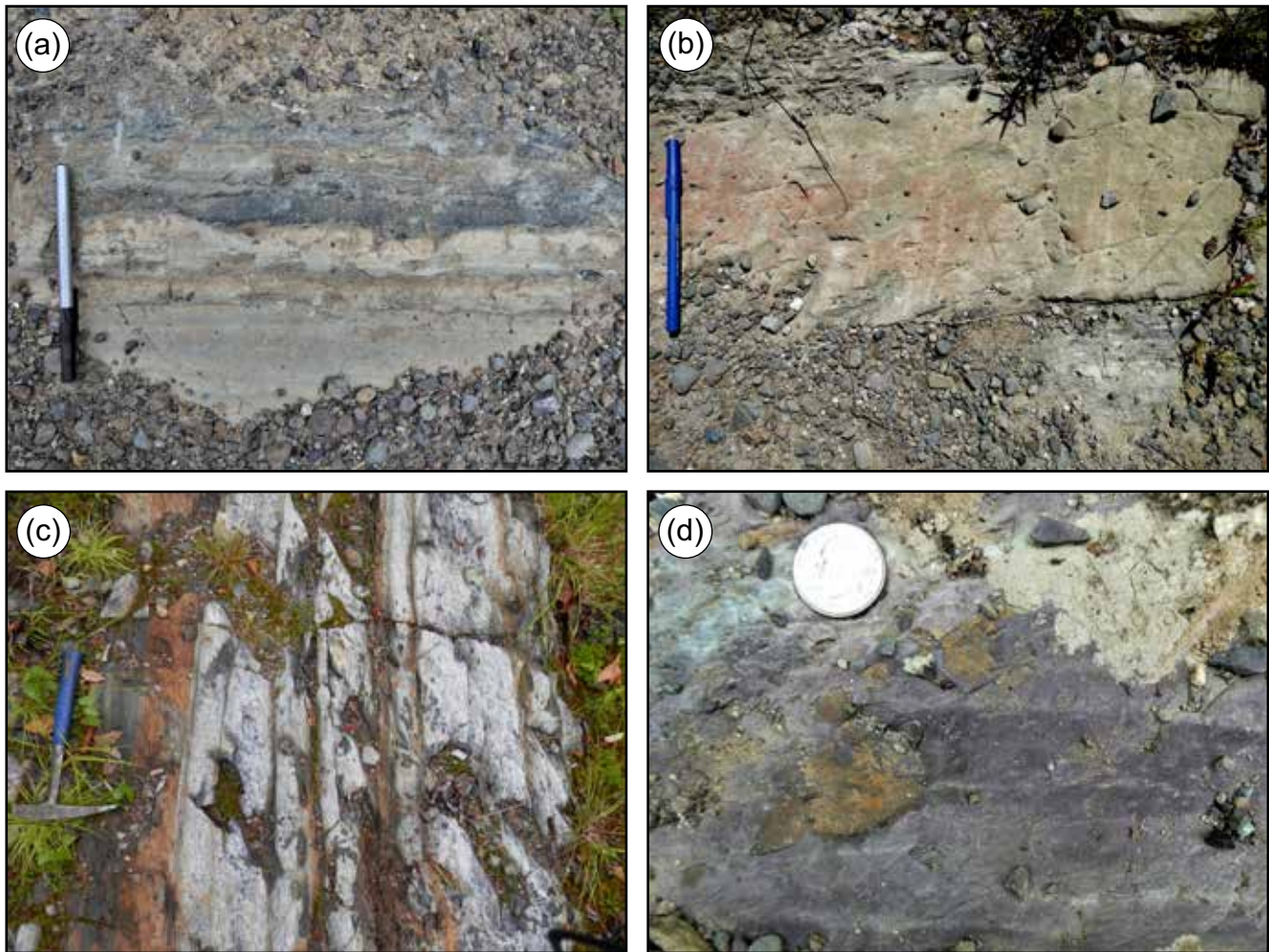irregular patches of calcite (Fig. 11f). This is interpreted as a peperite, a subaqueous ashflow combining ash and unlithified sediment.

COMPOSITION OF MAINE MIRAMICHI VOLCANIC ROCKS

Analytical methods

Seventeen samples of Olamon Stream volcanic rocks were collected in 2019 and sent to Activation Laboratories Ltd. in Ancaster, Ontario, for preparation and analysis of major elements by induction coupled plasma optical emission spectroscopy, and trace elements by induction coupled plasma mass spectrometry. Fifteen samples of least altered volcanic

rocks from the Danforth segment had been collected by Sayres (1986), prepared at Queens College, and analyzed at X-ray Assay Laboratories Ltd (Don Mills, Ontario) by X-ray fluorescence. Five additional samples from the Danforth segment were also processed by Activation Labs in 2014.

Results

Thirty-eight samples were selected for major element geochemistry from the volcanic rocks in the Greenfield and Danforth segments of which 18 contain trace element compositions and 22 have rare earth element compositions (Appendix A). For samples collected in this study the Universal Transverse Mercator (UTM) locations are recorded in Appendix B. Locations for previous samples collected from the Danforth segment are recorded in Sayres (1986). Volcanic rock types range from basalt to basaltic andesite, andesite, dacite, and rhyolite (Fig. 12), mirroring the textural variety shown in Figures 9, 10, and 11. Overall, rocks in the two segments exhibit similar compositions and proportions although, as mentioned earlier, mafic rocks present

Ludman et al. – Age, chemistry, and tectonic setting of Miramichi terrane (Early Paleozoic) volcanic rocks, eastern and east-central Maine, USA

Copyright © Atlantic Geology, 2021

Figure 11. Olamon Stream Formation mafic member. **(a)** Photomicrograph of porphyritic basaltic lava with fresh pyroxene and saussuritized plagioclase phenocrysts in a fine-grained crystalline matrix, viewed under crossed polars. **(b)** Photomicrograph of fresh pyroxene phenocrysts in a fine-grained pyroxene-plagioclase matrix, viewed under crossed polars. **(c)** Greenstone with pyroxene and plagioclase phenocrysts in chloritized matrix, viewed under plane-polarized light. **(d)** Mafic agglomerate with mostly endogenous fragments with lighter (more felsic) exotic clasts. **(e)** Mafic agglomerate with a highly chloritized matrix with endogenous and exotic clasts. **(f)** Peperite: mixed crystal-lithic mafic tuff, dark red baked mudstone fragments, and large calcite patches.

LUDMAN ET AL. – Age, chemistry, and tectonic setting of Miramichi terrane
(Early Paleozoic) volcanic rocks, eastern and east-central Maine, USA
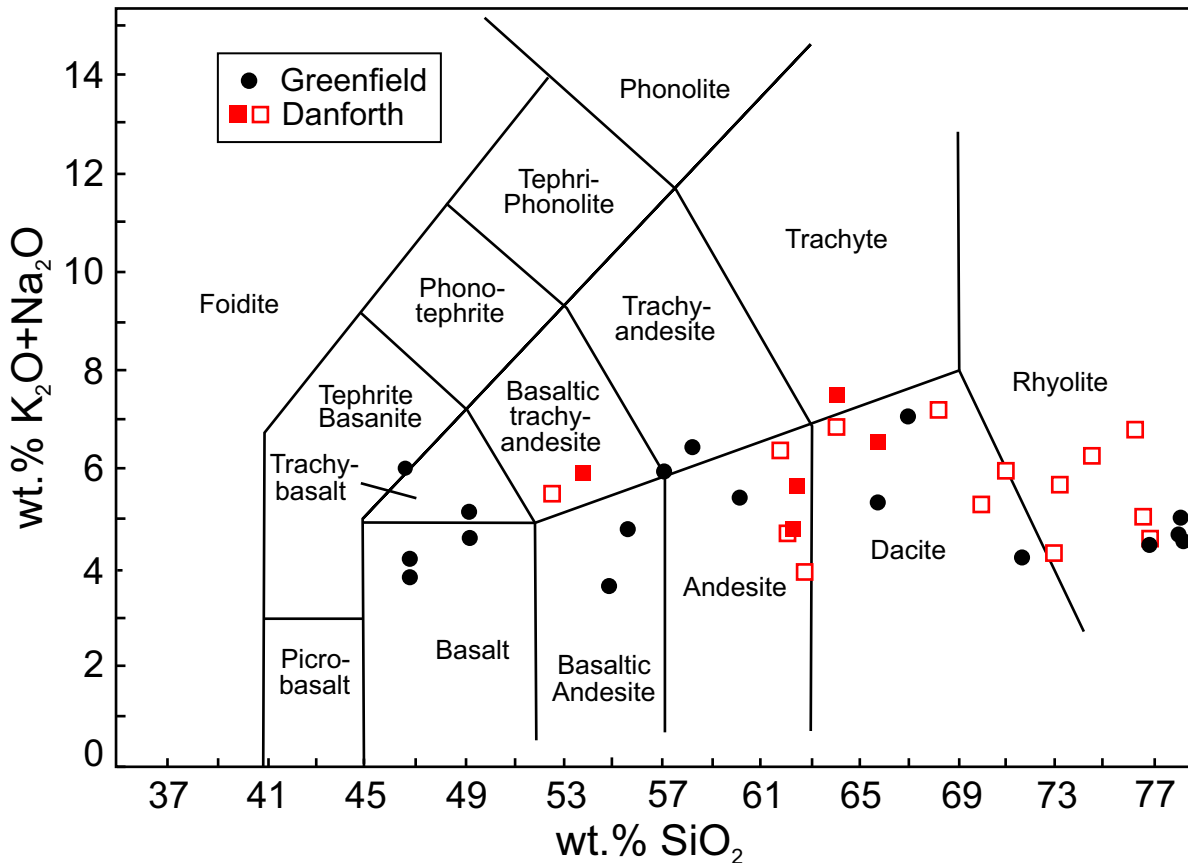
Copyright © Atlantic Geology, 2021

Figure 12. Classification of Miramichi volcanic rocks from the Greenfield and Danforth segments (after LeBas *et al.* 1986). Filled circles and squares – analysis by fusion ICP-OES, empty squares = analysis by XRF (after Sayres 1986).

in the Olamon Stream Formation are absent from the Stetson Mountain Formation. At this time, several explanations are plausible for this difference: different eruptive histories at different volcanic centers; different erosional levels in the two segments (although the bases of both can be observed, the top of neither is exposed); and structural complexities.

Sayres (1986) interpreted an internal stratigraphic sequence based on texture and eruptive style in the Danforth segment in an area with excellent outcrop control. However, no systematic compositional trend is apparent in the Stetson Mountain Formation, as andesite, dacite, and rhyolite are found in similar abundance in the lower and upper parts of the formation, commonly in the same outcrop. Similar combinations of intermediate and felsic rocks at individual outcrops are also common in the Olamon Stream Formation (e.g., Appendix A, samples 18B37a, b).

AGE OF MIRAMICHI VOLCANIC ROCKS IN MAINE

Analytical methods

Nine representative Miramichi volcanic rocks were collected for U–Pb dating in the summer of 2019, three each from the mafic member and main body of the Olamon Stream Formation, and three from the Stetson Mountain Formation. These samples were sent to Overburden Drilling Management, Ltd., Ottawa, Canada, for electric pulse disaggregation and initial zircon separation. Further separation and hand picking were carried out at the University of New Brunswick geochronology laboratory in Fredericton, New Brunswick, Canada.

U–Pb analyses were conducted at the University of New Brunswick using an ASI M-50 193 nm excimer laser ablation system (Complex Pro 110) with a 20 ns pulse width. The ablation system is equipped with a Laurin Technic Pty S–155 two–volume ablation cell coupled, using 4mm OD Nylon tubing, to an Agilent 7700× quadrupole ICP-MS equipped with dual external rotary pumps. Ablated material was transported to the ICP-MS using a mixed He (300 mL/min) and Ar (930 mL/min) carrier gas. Sensitivity was enhanced using the second external rotary pump and adding N_2 (2.0 mL/min) downstream of the cell. Due to isobaric interference of ^{204}Pb with ^{204}Hg impurities within the carrier gas, direct measurement of the ^{204}Pb signal was permitted by using in-line high-capacity Vici Metronics Hg traps on all gas lines ensuring that ^{204}Hg remains <150 cps under maximum sensitivity conditions. Correction of the ^{204}Hg interference on ^{204}Pb was then performed via peak–stripping using the measured ^{202}Hg on the gas background and assuming a canonical value for $^{202}Hg/^{204}Hg$.

Analyses of all unknowns were bracketed with at least 16

LUDMAN ET AL. – Age, chemistry, and tectonic setting of Miramichi terrane
(Early Paleozoic) volcanic rocks, eastern and east-central Maine, USA

Copyright © Atlantic Geology, 2021

spots on primary reference material to monitor and correct for instrument drift and time-dependent down-hole fractionation. For zircon, FC-1 (ca. 1099 Ma; Paces and Miller 1993) was used as primary external standard and accuracy was checked using Plesovice (ca. 337 Ma; Sláma *et al.* 2008) or GSC z1242 (ca. 2679 Ma; B. Davis personal communication 2021) A 17 μm crater size, 3 J/cm² laser energy, and a repetition rate of 4 Hz were used for all unknowns and standards. ^{90}Zr was used as a guide mass for ablations and internal standardization using an estimated value of 47 wt% Zr. NIST 610 was used for instrument tuning and as a concentration standard. Drift was modeled using Iolite3.7™ automatic fit function whereas down-hole fractionation was modeled using the automatic exponential fit option. The net ^{204}Pb (cps) signal was used for common Pb corrections (if required) for zircon and incorporated into the VizualAge U–Pb data reduction scheme (DRS) (Petrus and Kamber 2012) operating under Iolite3.7™. The routine uses an age estimate based on the measured ^{206}Pb/^{238}U and common Pb ratios based on the evolution curves of Kramers and Tolstikhin (1997). Common Pb corrections were applied only to zircon analyses with net ^{204}Pb >50 cps and 1σ internal errors <30%. All other data remained uncorrected.

Three volcanic rocks from the Olamon Stream Formation upper member yielded enough zircon grains for valid dating (Table 2). They include only two of the nine collected in 2019, dated by LA-ICPMS, and one dated earlier by U–Pb SHRIMP (Ludman *et al.* 2018). Concordia diagrams and images of zircons from the two new ages are shown in Figures 13 a and b. The UTM locations and the complete analytical data for the new dates are given in Appendix B and C. Unfortunately, none of the Danforth segment samples could be dated and the age of the Olamon Stream basalts is still uncertain.

The three ages are essentially identical, indicating eruption of the upper member of the Olamon Stream Formation at about 469 Ma, the boundary between the Lower and Middle Ordovician series (Floian–Dapingian stages). Unfortunately, they offer no insight into the timing of initial volcanism or the internal stratigraphy of the formation.

Attempts to date Olamon Stream basalts were inconclusive. Only one sample (20A8) had enough zircon grains to be dated, and most of these grains yielded a range of inheritance ages (Fig. 13c). Two zircon analyses close to Concordia *suggest* an age similar to those of the dated samples but are not conclusive.

DISCUSSION

Field, geochemical, and geochronologic data permit interpretation of the tectonic setting of Miramichi volcanic rocks in Maine, their correlation with volcanic units from both New Brunswick and other Cambrian–Ordovician Ganderian inliers in Maine, and a test of proposed tectonic models.

Tectonic setting

Miramichi volcanic rocks in Maine are a classic calc-alkaline basalt-andesite-rhyolite suite (Fig. 14a), associated with a subduction-related volcanic arc (Fig. 14b), consistent with previous interpretations of Miramichi volcanism (e.g., Sayres 1986; Winchester *et al.* 1992; van Staal *et al.* 2016). Niobium, lanthanum, and ytterbium data further suggest eruption in an ensialic continental arc rather than an oceanic setting (Fig. 14c). Lava flows, ashfall and ashflow tuffs, and volcanic agglomerates indicate recurrent Plinian and phreatomagmatic eruptions consistent with this environment.

Correlation of Miramichi volcanic rocks in Maine

Stratigraphic, lithologic, chemical, and geochronological data presented above permit correlation of the Olamon Stream and Stetson Mountain formations with volcanic rocks of the Miramichi inlier in New Brunswick and the Weeksboro–Lunksoos Lake and Munsungun Cambrian–Ordovician inliers in northern Maine. Direct connections are not possible with northern Maine inliers because of the extensive cover rocks, nor with the New Brunswick Miramichi volcanic rocks because the Pokiok plutonic suite at the New Brunswick–Maine border separates the Danforth segment from potential correlatives in west-central New Brunswick.

Structural complexities also obscure Maine–New Brunswick correlation. The Miramichi inlier is separated everywhere from adjacent Late Ordovician to Late Silurian strata

Table 2. Ages of Olamon Stream rhyolite, andesite, and dacite. Numbers in parentheses are original field stops. Oosu = Olamon Stream upper member; Oos float block traceable to Olamon Stream Formation but with uncertain stratigraphic position.

Specimen	Stratigraphic unit	Lithology	Age (Ma)
20A13 (18B70)	Oosu	Fine-grained andesitic crystal tuff	470 ± 4[1]
20A15 (19A61)	Oosu	Microporphyritic rhyolite tuff	467 ± 4[1]
13A78	Oos	Dacitic lava flow	469.3 ± 4.6[2]

Notes: [1]LA-ICPMS, University of New Brunswick Geochronology Lab; [2]USGS/Stanford SHRIMP; OS-1 in Ludman *et al*. 2018.

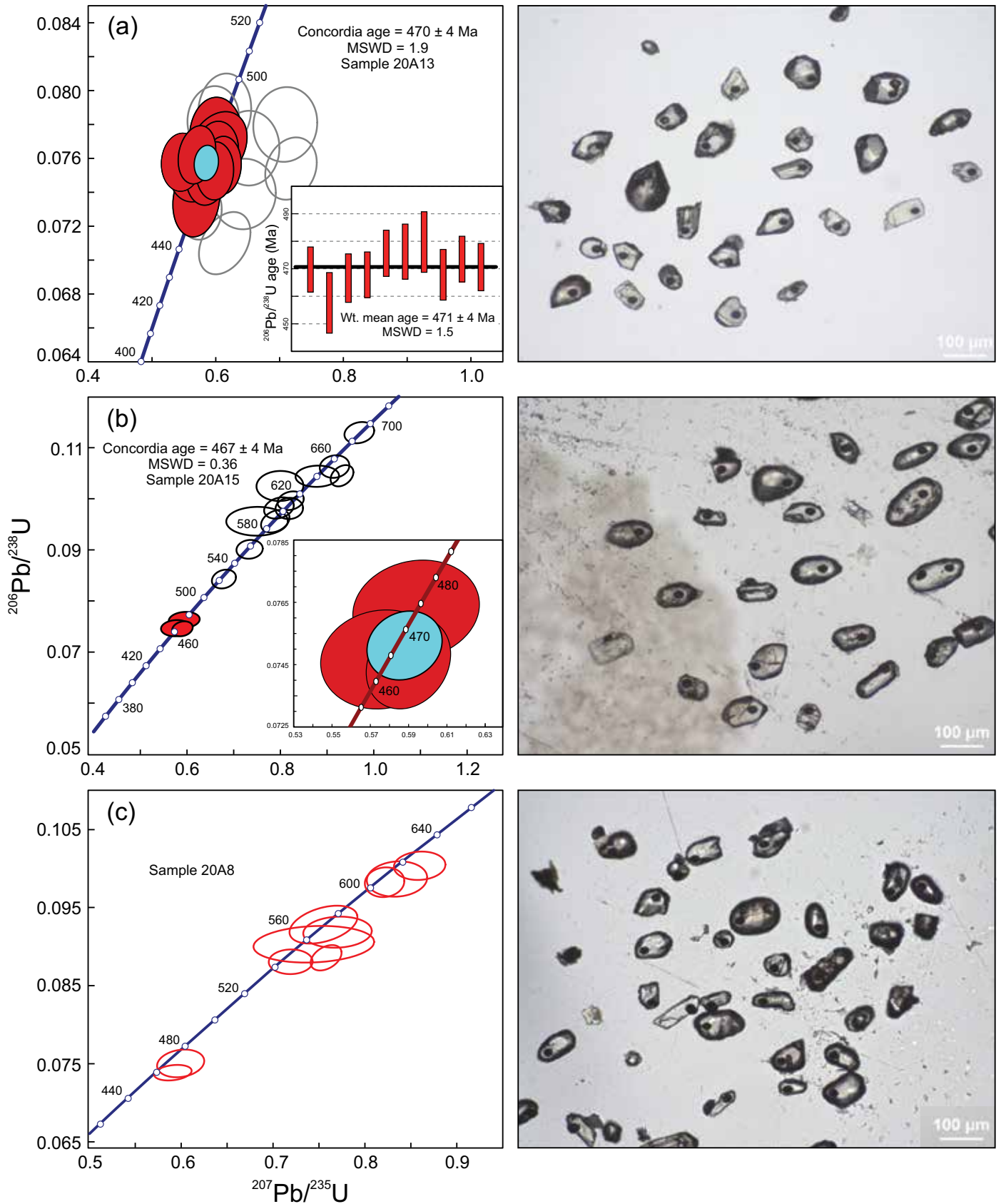**Figure 13.** Concordia diagrams and zircon images for Greenfield segment rocks. Error ellipses are 2σ. (a) Andesitic crystal tuff. (b) Microporphyritic rhyolitic tuff. (c) Basalt with insufficient data for precise dating.
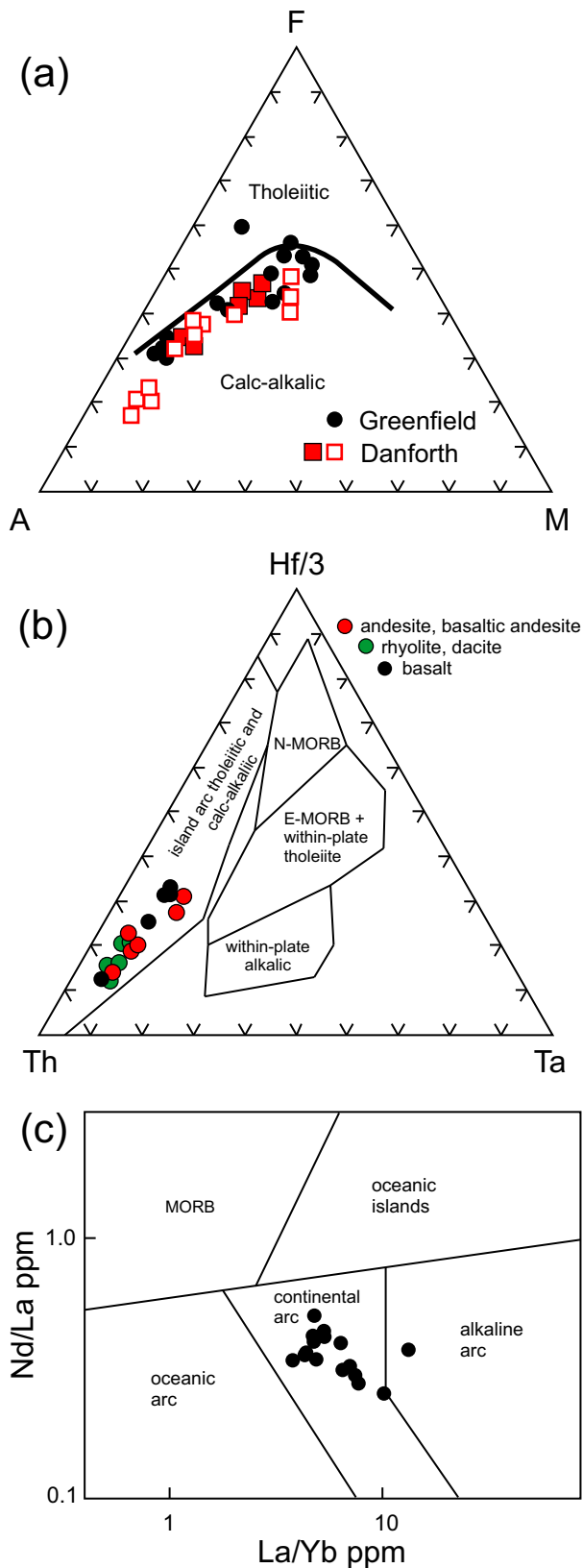
LUDMAN ET AL. – Age, chemistry, and tectonic setting of Miramichi terrane (Early Paleozoic) volcanic rocks, eastern and east-central Maine, USA

Copyright © Atlantic Geology, 2021

Figure 14. Tectonic setting of Miramichi volcanic rocks in the Danforth and Greenfield segments. (a) AFM diagram (after Irvine and Baragar 1971). (b) Hf/3-Th-Ta diagram (after Woods *et al.* 1979). (c) Nb/La-La/Yb diagram (after Pearce *et al.* 1984).

by regional-scale boundary faults and is cut into discrete blocks by internal faults that had complex thrust, high-angle dip-slip, and strike-slip episodes (Fig. 15; Ludman in press). The Bottle Lake and Pokiok complexes also interrupt continuity of these faults, adding another element of uncertainty to correlations. Indeed, depending on how the faults are connected through the Pokiok plutonic suite, otherwise strong candidates for correlation may lie in different fault blocks.

Thus, although areas of Early to Middle Ordovician Miramichi volcanic rocks in Maine and New Brunswick are parallel to the fault-controlled trend of the terrane, their component rocks may not actually be on strike with one another. Figure 15 shows one of several possible connections of Miramichi faults in Maine and New Brunswick. This model was chosen so that the Greenfield and Danforth segments are within the same fault block, but as a result, the Meductic Group in the Eel River are lies on another.

New Brunswick correlations

The most likely Stetson Mountain and Olamon Stream correlatives in New Brunswick include volcanic rocks of the Bathurst Supergroup in northern New Brunswick, the Meductic Group in west-central New Brunswick, and the Poplar Mountain volcanic complex that spans the New Brunswick–Maine border just north of Danforth (Fig. 16; Chi and Watters 2002).

The Bathurst Supergroup comprises volcanic and sedimentary rocks of the Tetagouche, Sheephouse Brook, and California Lake groups that occur in three stacked nappes of the Bathurst subduction complex (van Staal *et al.* 2016). Although ages of basal volcanic units in these groups overlap partially with those of the Olamon Stream Formation they are not considered correlative because they have within-plate signatures and are interpreted to have erupted in a back-arc environment associated with the Popelogan arc rather than the arc itself (e.g., van Staal *et al.* 2016; see below). In addition, most of its rocks are significantly younger than the dated Olamon Stream Formation samples.

The Poplar Mountain volcanic complex is geographically closest to the Stetson Mountain Formation, separated by a terrane-bounding fault from the Danforth segment only a few miles north of Danforth. At ca. 359 Ma (Chi *et al.* 2008), it is also significantly younger (10 myr) than the dated Olamon Stream Formation and its bimodal basalt–rhyolite suite suggests a back-arc rather than arc environment. We suggest that the Poplar Mountain volcanic rocks more likely correlate with interbedded rhyolite and basalt in the upper part of the Bathurst Supergroup (Sullivan and van Staal 1996).

Meductic Group correlation: Several previous workers (e.g., Fyffe 2001; Winchester *et al.* 1992; Ludman 2003; van Staal *et al.* 2016) have correlated the Stetson Mountain Formation (and by inference the Olamon Stream Formation) with volcanic rocks of the Meductic Group in the Eel River area of west-central New Brunswick (Fig. 15). Their com-
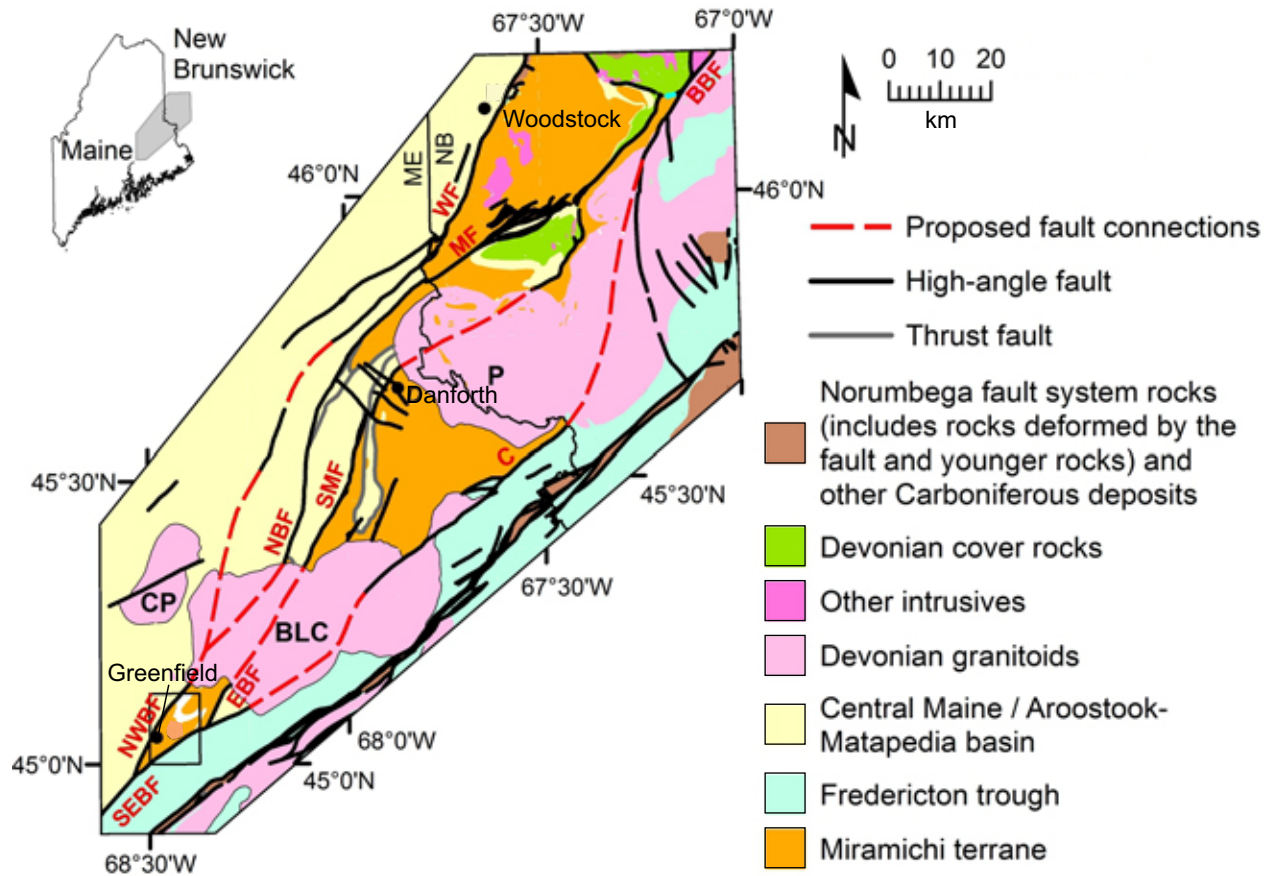
Figure 15. Proposed connections of boundary and internal Miramichi faults in Maine and New Brunswick, modified after Maine bedrock map (Osberg *et al.* 1985; updated) and digital data for New Brunswick 1:50 000 bedrock maps (Fyffe 2005; Fyffe *et al.* 2005a, b; Lutes, 2005; Lutes *et al.* 2005; Smith and Fyffe 2006a, b). Explanation is as in Figure 3, plus: BBF = Bamford Brook fault; MF-Meductic fault; WF-Woodstock fault.

mon location at the western margin of the Miramichi terrane, comparable stratigraphic positions (Fig. 17), compositions (Fig. 18), and interpreted tectonic settings provide compelling evidence for this correlation:

Stratigraphic position: Maine Miramichi and Meductic Group volcanic rocks erupted conformably on very similar substrates and are overlain unconformably by similar sedimentary rocks (Fig. 17). The oldest Miramichi unit in Maine is the Cambrian–Ordovician Baskahegan Lake Formation, (Ludman 1991, 2003), a distinctive sequence of quartzose and quartzofeldspathic sandstone with subordinate pelitic rocks. It is overlain conformably by quartzose sandstone and anoxic black shale of the Bowers Mountain Formation, and that, in turn, by the Olamon Stream and Stetson Mountain formations. The substrate in the Eel River area is the Woodstock Group, containing the Baskahegan Lake Formation, conformably and gradationally overlain by anoxic shale and sandstone of the Bright Eye Brook Formation, and then, conformably and gradationally, by the Porten Road Formation, the oldest volcanic unit in the Meductic Group (Fyffe 2001; McClenaghan *et al.* 2006).

Rocks interpreted to lie unconformably above the two volcanic suites (Fig. 17) are also similar to one another. The

Belle Lake Formation in New Brunswick (Fyffe 2001) and the Mill Priveledge Brook Formation in Maine are nearly identical, both consisting of sandstone interbedded with black shale and siltstone.

Similar substrate-volcanic relationships occur in the Bathurst Supergroup in northern New Brunswick, but with an important difference. Unlike the conformable sequences in the Eel River, Danforth, and Greenfield areas, a widespread unconformity attributed to the Penobscot orogeny separates, for example, the Miramichi Group substrate [Chain of Rocks (≈ Baskahegan Lake) + Knights Brook and Patrick Brook (≈ Bowers Mountain/Bright Eye Brook)] from volcanic and sedimentary rocks of the Tetagouche Group. The significance of this difference is discussed below.

Composition: The basalt-basaltic andesite-dacite-rhyolite suite in the Stetson Mountain and Olamon Stream formations is mirrored by the Meductic Group (compare Figures 18 and 12), but lithologic proportions are different and a well-defined temporal increase in mafic volcanism from the Porten Road to the Oak Mountain Formation is not recognized in Maine, although internal stratigraphy is less well established there. Based on the area, basalt is the most abundant lithology in the Eel River area (McClenaghan *et*
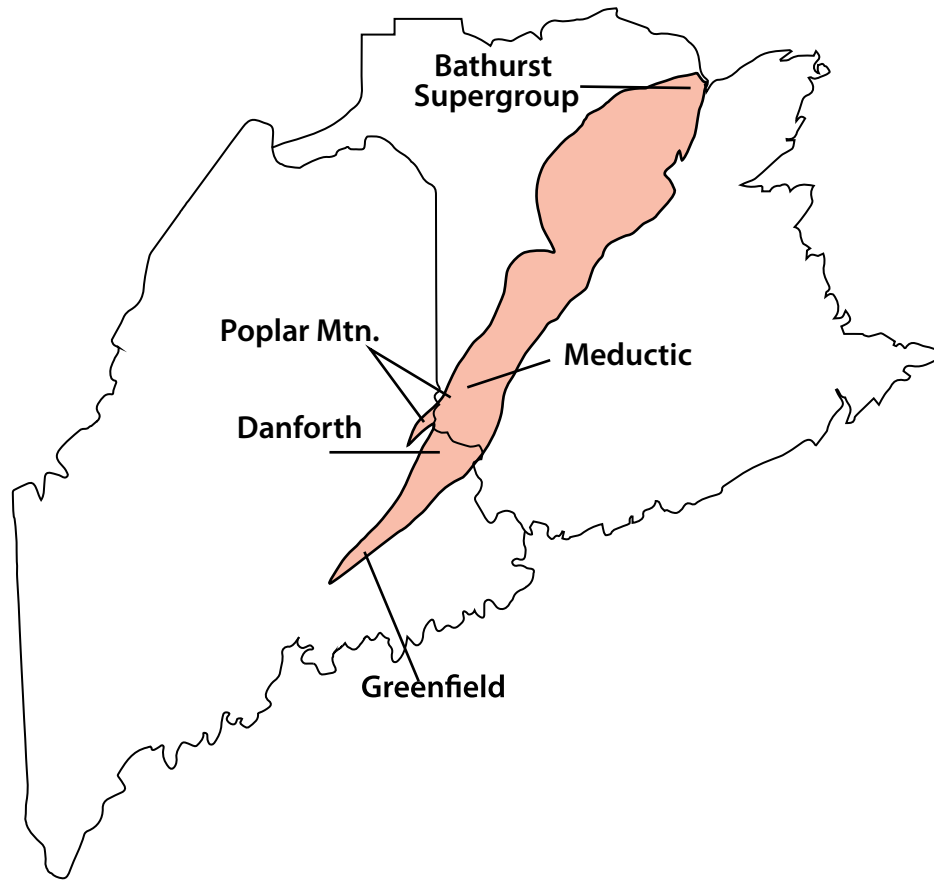
Ludman et al. – Age, chemistry, and tectonic setting of Miramichi terrane (Early Paleozoic) volcanic rocks, eastern and east-central Maine, USA

Copyright © Atlantic Geology, 2021

Figure 16. Locations of potentially correlative Early to early Middle Ordovician volcanic rocks of the Miramichi inlier.

al. 2006) and occur in all three Meductic Group volcanic formations but are absent from the Danforth segment and are a very minor component of the Greenfield segment, as discussed above.

Tectonic setting: Both the Meductic Group (Winchester *et al.* 1992; McClenaghan *et al.* 2006) and Maine Miramichi volcanic suites are calc-alkaline. Common siliciclastic substrates and trace element discrimination diagrams further attribute volcanism in both suites to subduction-related continental arcs.

Age: Early Ordovician graptolites in the underlying Bright Eye Brook and Middle Ordovician graptolites in the overlying Belle Lake formations constrain the Meductic Group volcanic rocks to the late Early Ordovician to Early Middle Ordovician (Fyffe 2001; R. Wilson, personal communication 2021). This corresponds to a span of ca. 477–458 Ma (Cohen et al 2013, updated 2021), that is compatible with the ca. 469 Ma age of the upper member of the Olamon Stream Formation but does not indicate correlation with any of the three Meductic Group volcanic units.

Equivalence of the Olamon Stream, Stetson Mountain, and Porten Road formations is suggested by their positions as the oldest volcanic units conformably overlying similar pre-volcanic substrates, and supported by the restriction of rhyolite, abundant in Maine, solely to the Porten Road Formation in the Meductic Group. However, detailed examina-

tion of the ages and geochemistry of the formations reveals inconsistencies that suggest another possibility.

For example, the dated Porten Road dacite (480 ± 3 Ma; Mohammadi *et al.* 2019) is 11 myr older than dated Olamon Stream rhyolite, dacite, and andesite (ca. 469 ± 4 Ma). It is important to note that the dated Olamon Stream Formation rocks are from its upper member, whereas the Porten Road age is from near the base of the formation and thus closest to the underlying Bright Eye Brook Formation. The age of the Olamon Stream lower member, stratigraphically comparable to the dated Porten Road sample, is unknown.

Porten Road volcanism could conceivably have spanned 11 myr, but in that case the progressive upward increase in mafic rocks in the formation would be expected to occur in the Olamon Stream Formation as well. L.R. Fyffe (personal communication 2021) reported that Olamon Stream andesites described above are more like those of the Eel River Formation than those of the Porten Road Formation, implying at least partial correlation with younger parts of the Meductic Group.

Comparison of the Olamon Stream and Stetson Mountain formations with the three Meductic group volcanic units reveals other inconsistencies. Lithologically, neither black shales abundant near the base of the Porten Road Formation nor polylithic debris flows reported in Porten Road and Eel River cores (McClenaghan *et al.* 2006) are observed
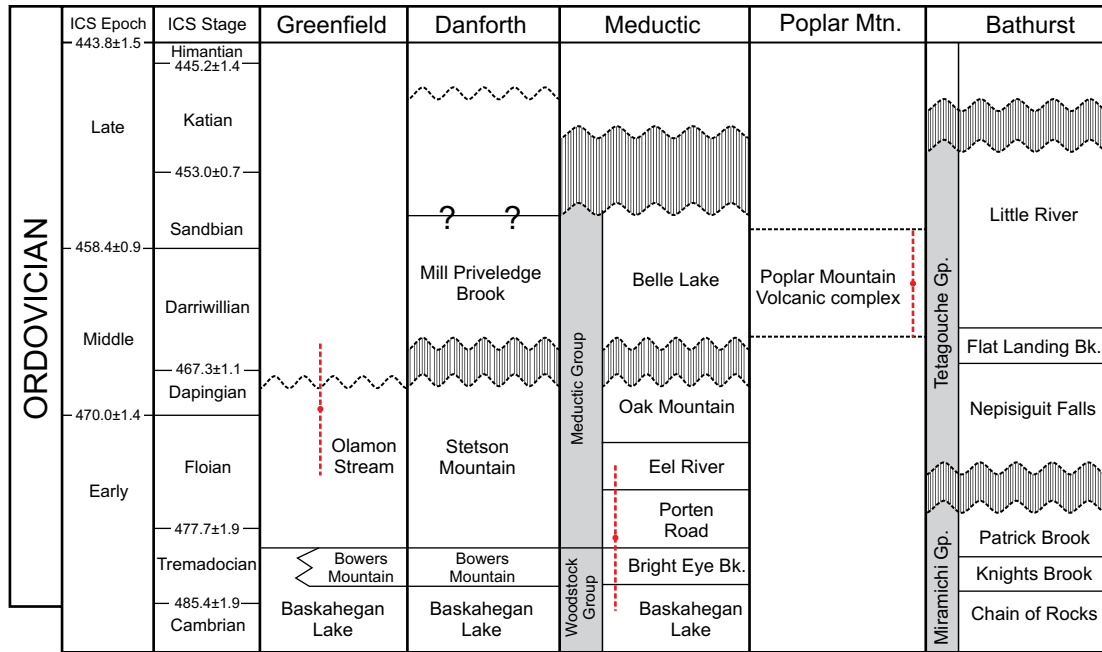

ICS Epoch	ICS Stage	Greenfield	Danforth	Meductic	Poplar Mtn.	Bathurst

Figure 17. Proposed relationships of Miramichi volcanic rocks in Maine with Miramichi volcanic rocks in New Brunswick. Red lines = range of U-Pb zircon dates: *Olamon Stream* (average of three dates reported above); *Meductic* (age of basal Porten Road Formation; Mohammadi *et al.* 2019) Stage boundary ages after Cohen *et al.* (2013, updated 2021).

in the Olamon Stream Formation. Chemically, Porten Road rhyolites have, on average, lower TiO_2, Fe_2O_3, Na_2O and P_2O_5 and higher Al_2O_3, MgO, and CaO than those of the Olamon Stream and Stetson Mountain formations. In addition, Porten Road rhyolite and dacite samples have different rare earth element profiles (Figs. 19 a, b) and higher La/Yb ratios than those in the Olamon Stream and Stetson Mountain formations. Rare earth element profiles of Porten Road and Eel River andesite samples are also different from those of the Maine rocks (Fig. 19 c), as are those of Oak Mountain and Olamon Stream basalts (Fig. 19 d).

We suggest that the similarities outweigh the differences and that, absent ages for the Stetson Mountain Formation and the Olamon Stream lower and basalt members in Maine, and the Eel River and Oak Mountain formations in New Brunswick, only broad correlation with the Meductic Group is possible. A volcanic arc 350 km long is unlikely to exhibit simple "layer-cake" stratigraphy or uniform lithologic and chemical profiles along its length, and the lithologic and chemical differences described above may indicate eruptions at different volcanic centers in a Maine–Meductic arc.

Correlation with Cambrian–Ordovician belts in northeastern Maine

Large volumes of volcanic rock in the extensive Cambrian–Ordovician Weeksboro-Lunksoos Lake and Munsungun belts in Maine northwest of the Miramichi inlier (Fig. 1) had, until recently, been last studied at the dawn of the plate tectonic era (Neuman 1967; Hall 1970). Ongoing mapping by Wang (2018, 2019, 2021) and exploration at the Bald

Mountain (Munsungun) and Pickett Mountain VMS prospects (W-L) are yielding new insights into volcanism during accretion of the leading edge of Ganderia to Laurentia, and coupled with this study, the geometry of that accretion (see below).

Weeksboro–Lunksoos Lake inlier: Ordovician volcanic rocks in this belt, approximately 75 km northwest of the Danforth segment, are mapped as the Shin Brook Formation, host of the Pickett Mountain VMS deposit. Stratigraphic, lithologic, and geochronologic details reported by Neuman (1967) strongly support correlation of the Shin Brook with the Stetson Mountain and Olamon Stream formations (Fig. 20).

The Shin Brook volcanic rocks, now including greenstone mapped by Neuman (1967) and Wang (personal communication 2021), lie unconformably on the Cambrian–Ordovician Grand Pitch Formation, a thick sequence of quartzofeldspathic sandstone very similar to and correlated with Miramichi rocks now included in the Baskahegan Lake Formation (Larrabee *et al.*1965; Ludman 1991). Neuman (1967) attributed this discontinuity to a "Penobscot disturbance", now described as the Penobscot orogeny in northern Maine (Wang, 2018, 2019), and northern and eastern New Brunswick (van Staal et al. 2016). This relationship is unlike the relationships in the Maine Miramichi, and Eel River New Brunswick areas where Early Ordovician volcanic rocks lie conformably on a pre-volcanic anoxic substrate.

Early reports of the Shin Brook volcanic suite described dacitic and andesitic tuffs, breccias, agglomerates, and rare lavas overlain by basalt, based largely on petrographic

LUDMAN ET AL. – Age, chemistry, and tectonic setting of Miramichi terrane (Early Paleozoic) volcanic rocks, eastern and east-central Maine, USA

Copyright © Atlantic Geology, 2021
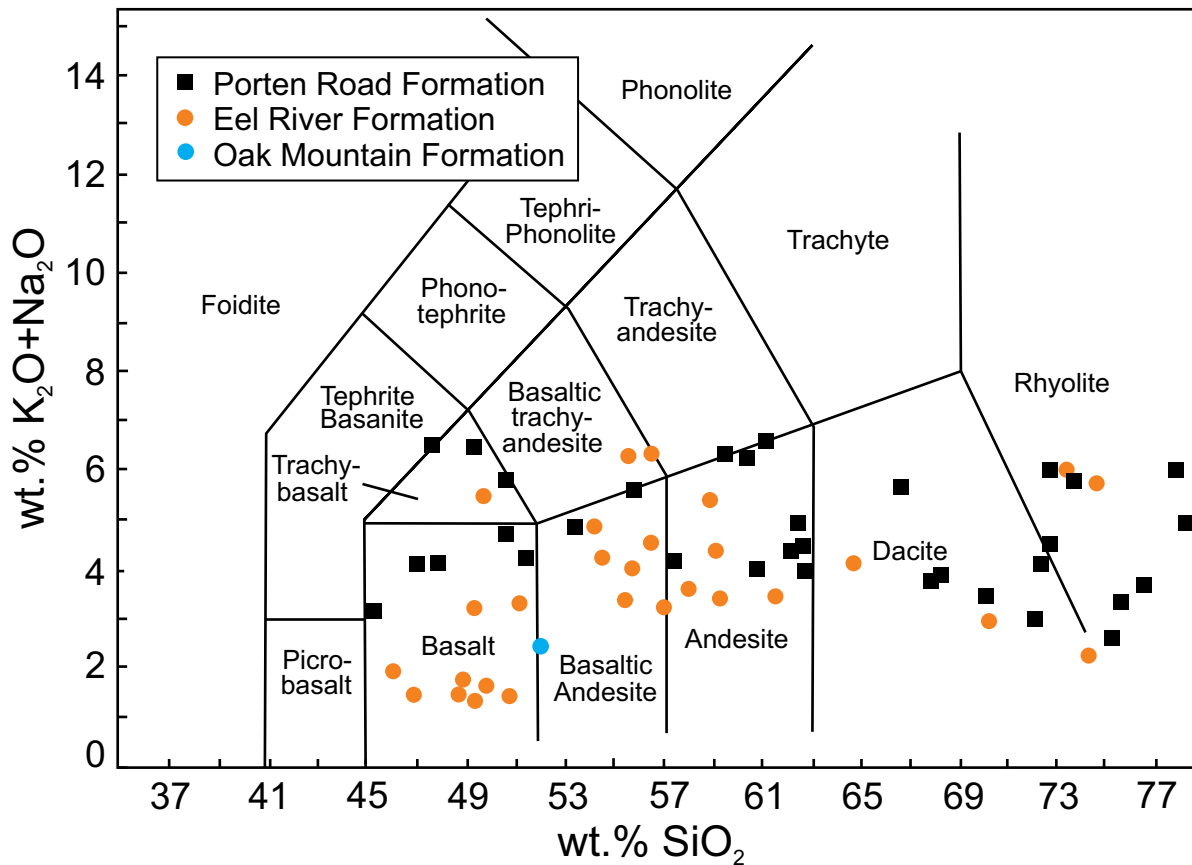
Figure 18. Chemistry of Meductic Group volcanic rocks (McClenaghan *et al.* 2006; after LeBas *et al.* 1986).

properties and only a few chemical analyses (Ekren and Frischknecht 1967; Neuman 1967). Recent chemical analyses from boreholes at the Pickett Mountain VMS deposit (formerly Chase Mountain) confirm a largely bimodal rhyolite-basalt suite with subordinate andesite intruded by subvolcanic felsic and mafic intrusions (McCormick 2021; C. Wang, personal communication 2021).

A rich trilobite and brachiopod faunal assemblage in intercalated volcaniclastic sedimentary rocks dates Shin Brook volcanism directly as late Early Ordovician to earliest Middle Ordovician (Neuman 1967) corresponding to ca. 470 to 458 Ma; Cohen *et al.* 2013, updated 2021). A 467 ± 5 Ma age for dacite reported by Ayuso *et al.* (2003) from the Pickett Mountain prospect was from a dyke that cuts the Shin Brook volcanic rocks and therefore serves as a minimum age for the formation. Preliminary ages of 484 ± 0.6 and 481 ± 0.6 Ma from that prospect suggest earlier volcanic activity (McCormick 2021) but need to be confirmed. The Weeksboro–Lunksoos Lake volcanic suite is thus partly older and partly coeval with the Miramichi volcanic rocks in Maine.

Munsungun inlier: The Munsungun inlier, about 50 km north of the Weeksboro–Lunksoos Lake belt, contains Early Ordovician volcanic rocks mapped in different parts of the inlier as the Munsungun Lake Formation and Round Mountain and Center Mountain volcanic suites (Wang 2018, 2019, 2021).

The early Ordovician volcanic rocks lie unconformably on the Chase Brook Formation, a Cambrian–Ordovician olistostromal mélange, a relationship similar to that in the Weeksboro–Lunksoos Lake inlier. Recent mapping indicates that this mélange can be traced to the northwest side of the Weeksboro–Lunksoos Lake inlier (C. Wang, personal communication 2021).

The Munsungun Lake Formation comprises mostly arc-related basalts intruded by subvolcanic diabase dykes and sills, with subordinate dacite and andesite. In contrast, the Round Mountain volcanic rocks are tholeiitic, primitive basalts exhibiting within-plate tectonic affinity (Wang 2021).

Munsungun inlier volcanic activity has also been dated as beginning at the boundary between the Early and Middle Ordovician: Munsungun Lake tuffs at 467 ± 4Ma (Ayuso *et al.* 2003), 471.2 ± 4.2 Ma (Wang 2019), and 468.2 Ma (Wang 2018). These ages indicate that calc-alkaline arc-related volcanism occurred simultaneously in the three Cambrian–Ordovician inliers in Maine, although to lesser extents in the northerly belts.

LUDMAN ET AL. – Age, chemistry, and tectonic setting of Miramichi terrane (Early Paleozoic) volcanic rocks, eastern and east-central Maine, USA

Copyright © Atlantic Geology, 2021
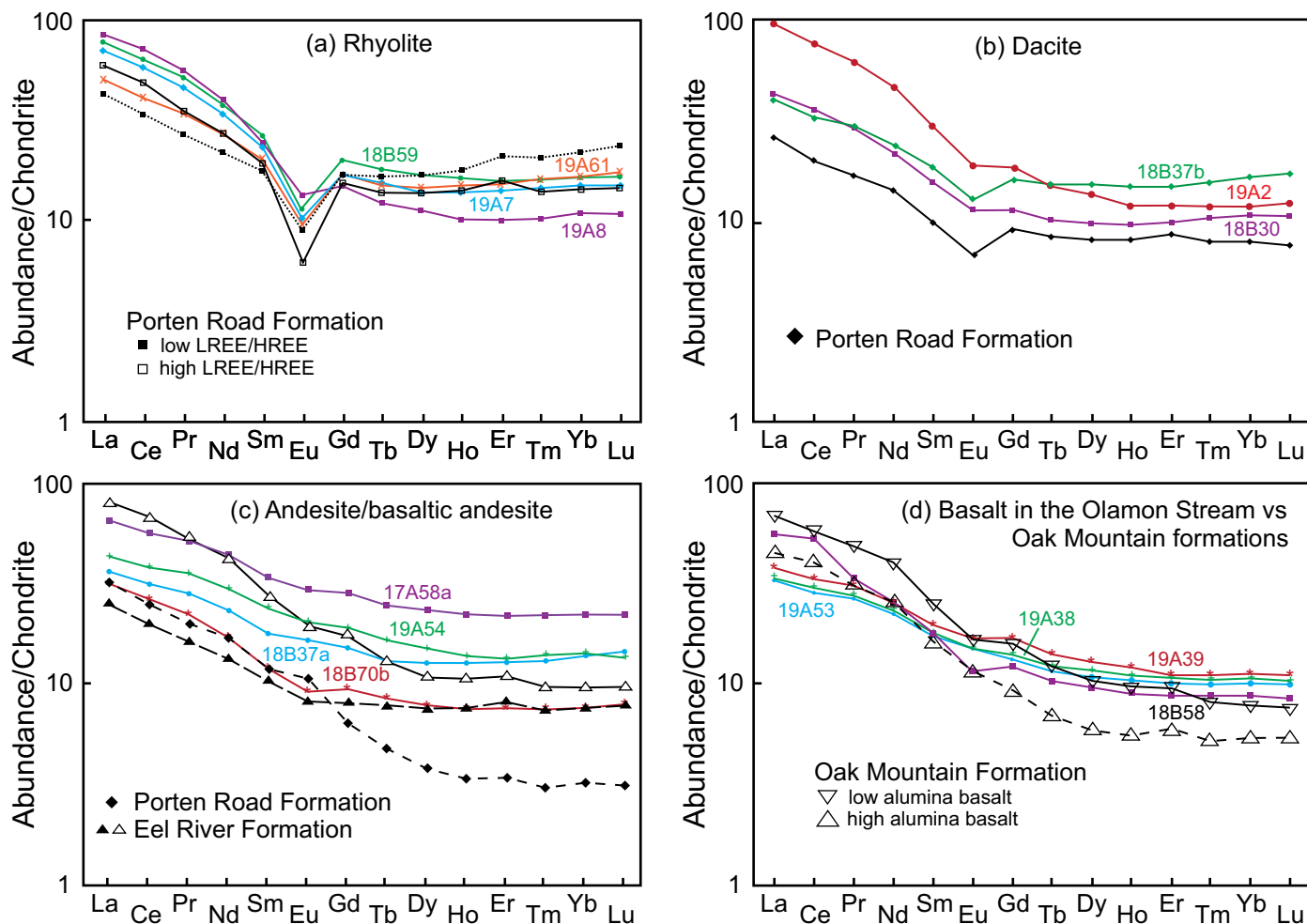
Figure 19. Comparison of rare earth element profiles in Maine (this paper) and Meductic Group volcanic rocks (Fyffe 2001). (a) Rhyolite. (b) Dacite. (c) andesite/basaltic andesite. (d) Basalt in the Olamon Stream vs Oak Mountain formations.

TECTONIC IMPLICATIONS

Middle Ordovician plate accretion: "Taconic" orogeny

Models for the timing and nature of events at the leading edge of Ganderia that first collided with Laurentia have been based largely on information from New Brunswick: the Miramichi and Elmtree inliers; the much smaller Popelogan inlier and even smaller Oxford Brook exposure to the west; and the Straughan Brook drill hole through the Carboniferous Maritimes Basin to the east (Fig. 1). Maine Miramichi volcanic data presented here, combined with new information from the extensive Weeksboro–Lunksoos Lake and Munsungun belts closer to that leading edge (Fig. 1), add significantly to our understanding of Ganderian accretion to Laurentia.

As described above, our geochemical data support the model of continental arc volcanism attributed to the Popelogan arc, and the Poplar Mountain volcanic suite is consistent with an intra-arc or back-arc rifting setting (Tetagouche Group), and subsequent closing of the back-arc basin (van Staal *et al.* 2016). That model proposed initial rollback of an eastward-dipping subducted slab beneath the Popelogan arc, accompanied by northwestward migration of arc volcanism, first to the Weeksboro–Lunksoos Lake inlier and eventually as far as the Munsungun inlier (Figs. 21a, b).

This model, however, is not consistent with simultaneous Floian–Dapingian volcanism in the three Maine inliers described above (Fig. 22), including at ca. 471–468 Ma in the Miramichi, Weeksboro–Lunksoos Lake and Munsungun inliers, and at ca. 480–484 Ma in the Meductic Group and possibly ca. 485–481 Ma in the Weeksboro–Lunksoos Lake inlier (Table 3). The current distance between the Miramichi and Munsungun inliers is about 150 km and although it is difficult to estimate the original span because of Ordovician extension and compression and Salinic and Acadian telescoping, it was almost certainly significantly greater than today.

Even the current 150 km span is much wider than can be explained by a single shallow eastward-dipping subduction zone. We therefore propose that simultaneous Ordovician volcanism in the three inliers indicates eruptions in two or perhaps as many as three subduction zones (Fig. 23), analogous to the Molucca–Celebes Sea collision zones (Hall and

Ludman et al. – Age, chemistry, and tectonic setting of Miramichi terrane (Early Paleozoic) volcanic rocks, eastern and east-central Maine, USA

Copyright © Atlantic Geology, 2021
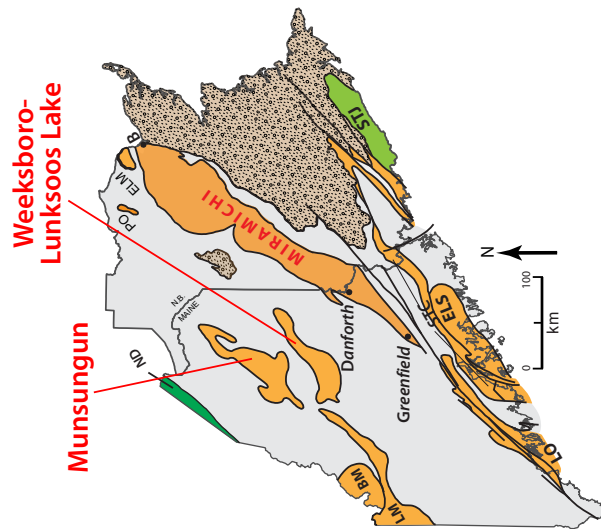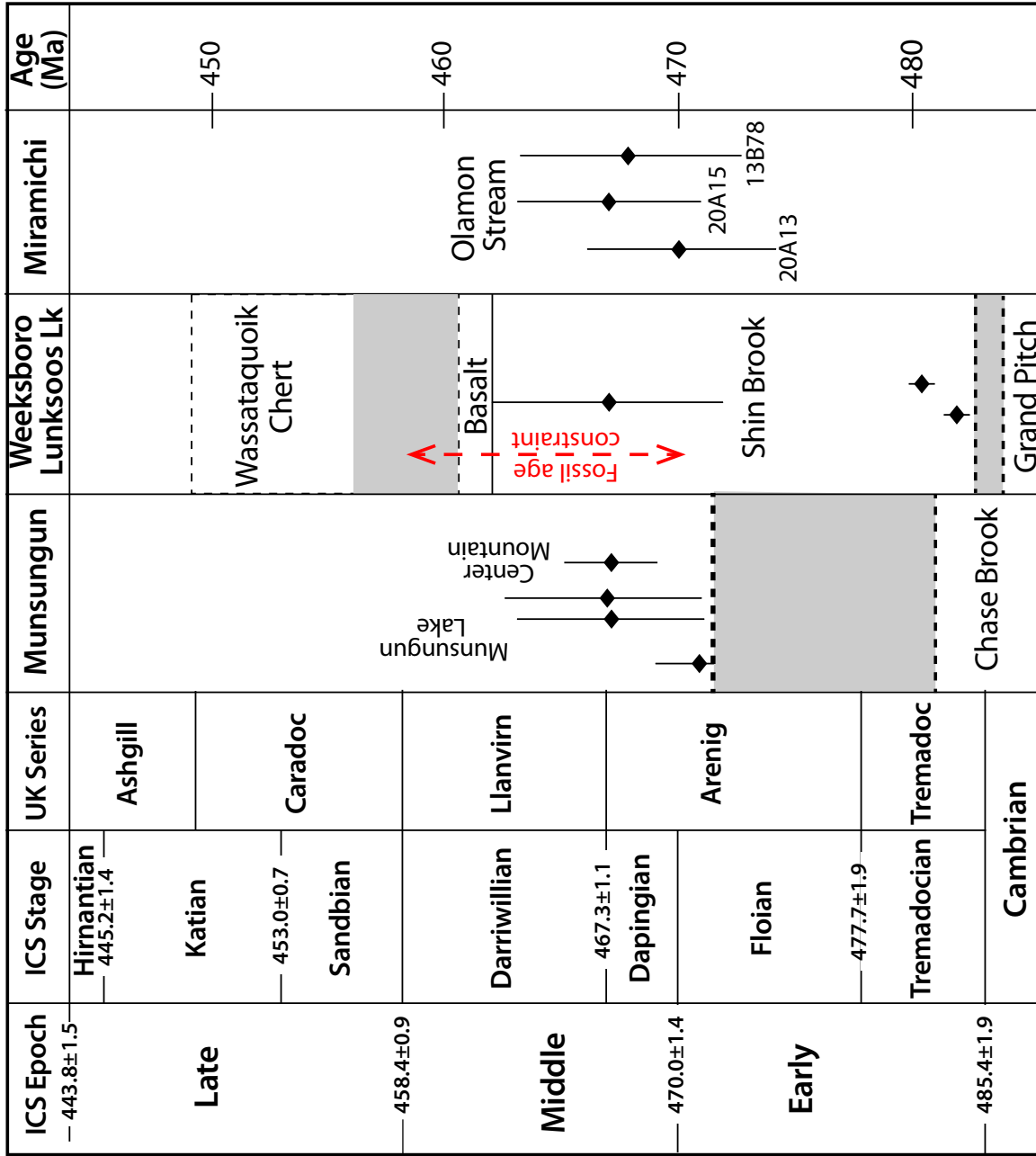
Figure 20. Geochronologic evidence for timing of Cambrian–Ordovician volcanism in eastern Maine. Abbreviations on inset map same as in Figure 1.

LUDMAN ET AL. – Age, chemistry, and tectonic setting of Miramichi terrane
(Early Paleozoic) volcanic rocks, eastern and east-central Maine, USA

Copyright © Atlantic Geology, 2021
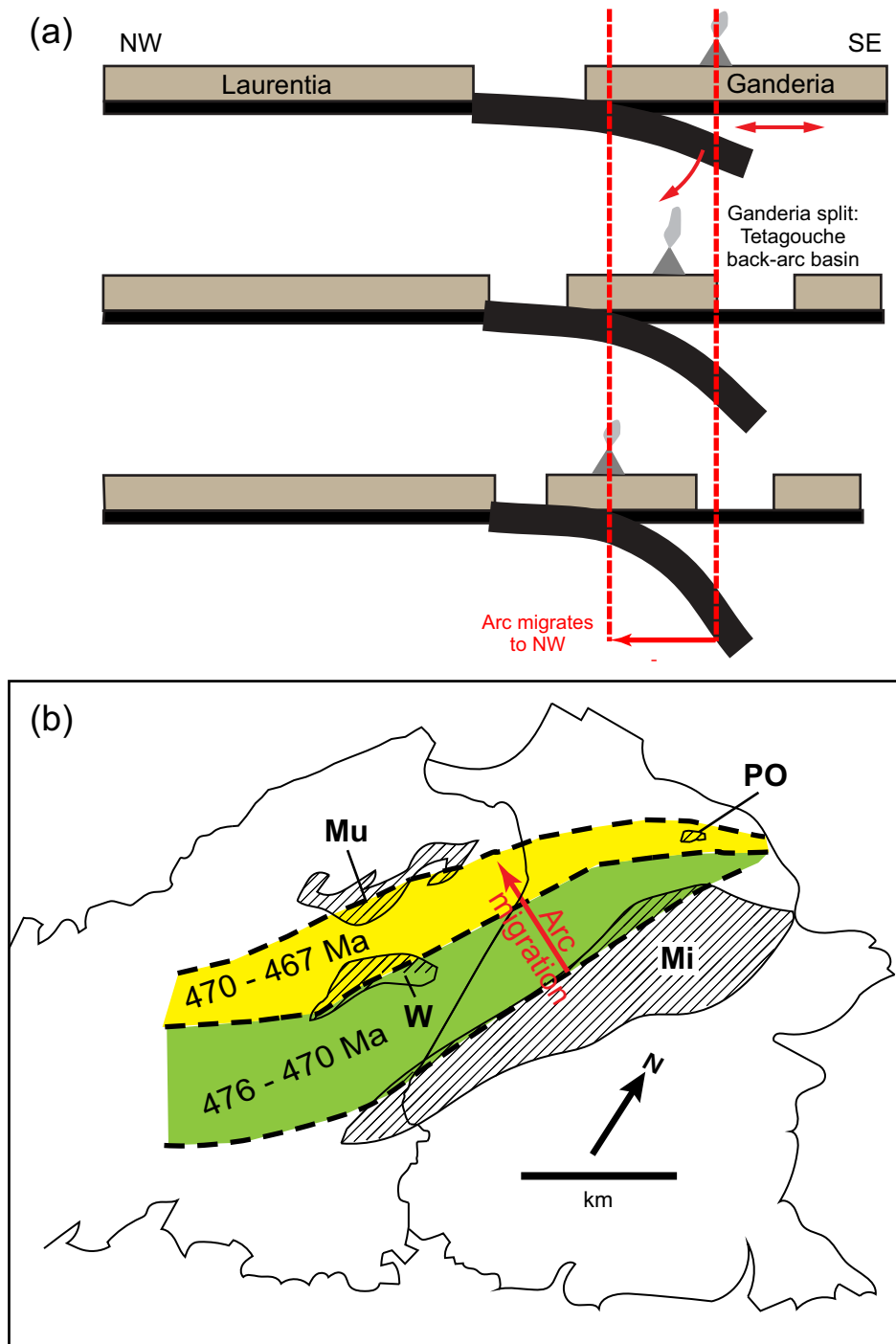
Figure 21. Arc migration model for Popelogan arc evolution (after van Staal *et al.* 2016). (a) Cross-Section showing initial moderate subduction, followed by arc migration and opening of the Tetagouche back-arc basin. (b) Map showing zones of proposed northwestward migration of the Popelogan arc. Abbreviations on inset map same as in Figure 1.

Nichols 1990). The largely bimodal nature of Weeksboro–Lunksoos volcanism suggests a third possibility: that it and the Munsungun rocks may represent an arc/back-arc system comparable to that of the Meductic/Tetagouche rocks.

The multiple arc model would be more convincing if there were associated melanges like that accompanying Penobscot arc closure in the Munsungun inlier, or subduction com-plexes like that in the Bathurst area. The absence of these features, however, does not preclude a subduction-related arc. For many years, their absence from the Eastport–Mas-carene volcanic belt in eastern Maine and southeastern New Brunswick prevented widespread acceptance of a subduc-tion model, but Llamas and Hepburn (2013) argued con-vincingly for eruption over a west-dipping subduction zone.

Ludman et al. – Age, chemistry, and tectonic setting of Miramichi terrane (Early Paleozoic) volcanic rocks, eastern and east-central Maine, USA

Copyright © Atlantic Geology, 2021
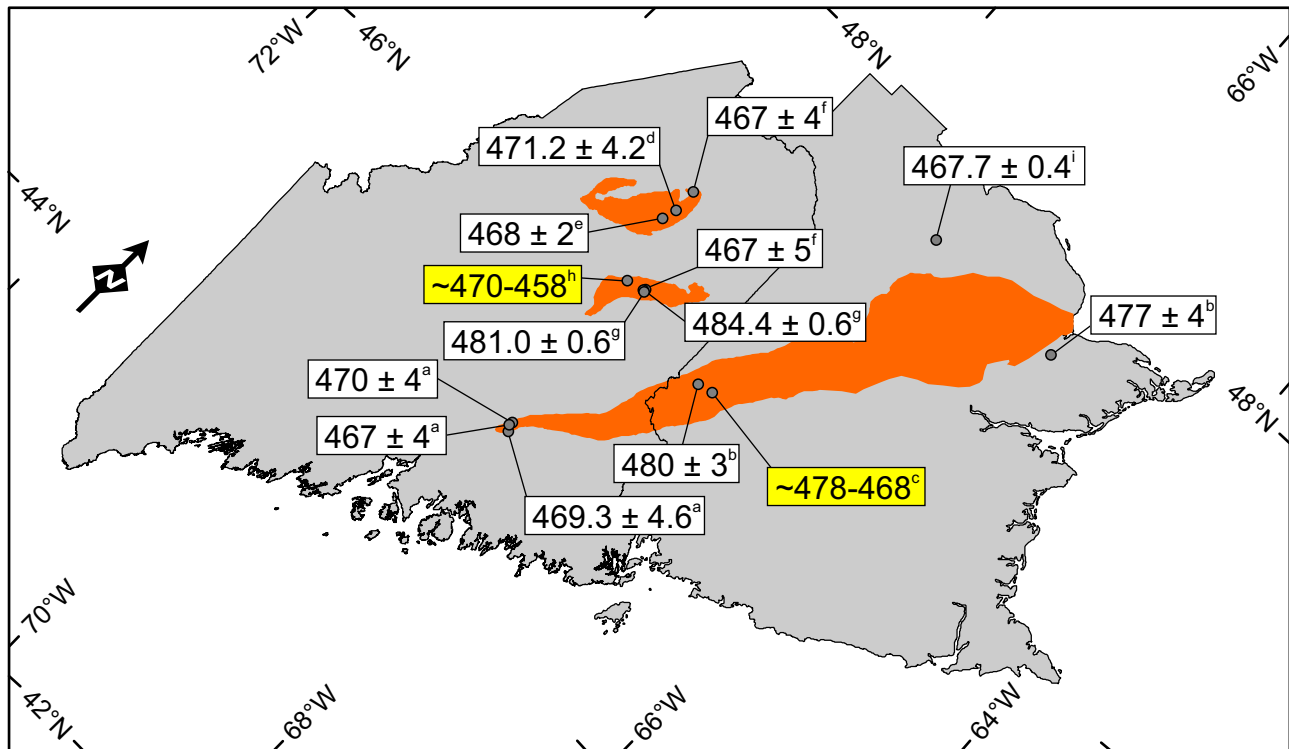
Figure 22. Map showing geographic distribution of dated Ordovician volcanic rocks in eastern Maine and west-central New Brunswick. Ages in millions of years (Ma). White boxes indicate U–Pb age control and yellow boxes indicate fossil-based age control.

Penobscot orogeny

Neuman (1967) was the first to recognize an unconformity in the Weeksboro–Lunksoos Lake inlier separating early Ordovician volcanic rocks (Shin Brook Formation) from the underlying Cambrian–Ordovician Grand Pitch Formation. This unconformity is now recognized in a broad area from the Munsungun inlier in northeastern Maine (Wang 2018), to northern (Bathurst area) and southeastern (Annidale area) New Brunswick and is attributed to a Penobscot orogeny related to early Ordovician terrane accretion on the trailing edge of Ganderia (Fyffe *et al.* 2011; van Staal *et al.* 2016).

This early Ordovician unconformity has not been rec-

Table 3. Sources of data for Figure 22. Italics indicate fossil age control. All others based on U–Pb zircon dating.

Datum	Age (Ma)	Stratigraphic unit	Source
a	470 ± 4	Olamon Stream Formation (upper member)	This paper
a	467 ± 4	Olamon Stream Formation (upper member)	This paper
a	469.3 ± 4.6	Olamon Stream Formation (float)	This paper
b	480 ± 3	Porten Road Formation	Mohammadi *et al.* (2019)
b	477 ± 4	Straughan Brook borehole felsic tuff	Mohammadi *et al.* (2019)
c	*(ca. 478–468)*	*Bright Eye Brook, Belle Lake formations*	*Fyffe (2001)*
d	471.2 ± 4.2	Munsungun Lake Formation	Wang (2019)
e	467 ± 4	Munsungun Lake Formation	Ayuso *et al.* (2003)
f	468.0 ± 2	Munsungun Lake Formation	Wang (2018)
f	467 ± 5	Dyke cutting Shin Brook Formation	Ayuso *et al.* (2003)
g	484.4 ± 0.6	Shin Brook Formation	McCormick (2021)
g	481.0 ± 0.6	Shin Brook Formation	McCormick (2021)
h	*(ca. 470–458)*	*Shin Brook Formation (Wassataquoik Chert)*	*Neuman (1967)*
i	467.7 ± 0.4	Goulette Brook Formation (Oxford Brook inlier)	van Staal *et al.* (2016)

Ludman et al. – Age, chemistry, and tectonic setting of Miramichi terrane (Early Paleozoic) volcanic rocks, eastern and east-central Maine, USA

Copyright © Atlantic Geology, 2021
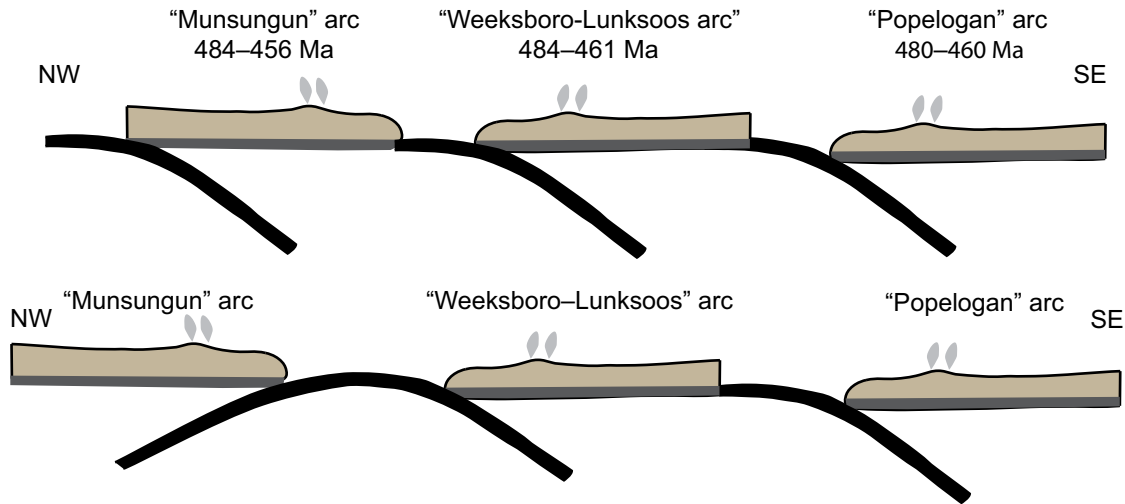
Figure 23. Two possible versions of a multiple arc model.

ognized, however, in the southwestern part of the Miramichi inlier in Maine and New Brunswick. Instead, there is a continuous and gradational transition upward from the Woodstock Group to the Meductic Group as described above (Fyffe 2001; McClenaghan *et al.* 2016). Contact relationships are less clear in Miramichi exposures in Maine, but the basal Baskahegan Lake and Bowers Mountain formations appear to have experienced the same deformation history as the overlying Olamon Stream and Stetson Mountain formations.

Its absence does not refute the existence of a Penobscot orogeny, nor its tectonic interpretation, but does suggest that its geographic impact was more complex than previously interpreted, and that additional work is necessary to explain its absence.

CONCLUSIONS

1. Volcanic rocks in the Danforth and Greenfield segments of the Miramichi inlier in Maine are dominantly pyroclastic andesite, dacite, and rhyolite, with subordinate lavas and agglomerates, and minor basalt only in the Greenfield segment.

2. Rocks from both segments are calc-alkaline, erupted in a continental-floored arc above a subduction zone.

3. U–Pb zircon dating indicates arc activity in the Greenfield segment around ca. 469 Ma, at the boundary between the early and middle Ordovician (Floian–Dapingian), corresponding to the Meductic phase of Popelogan arc development.

4. Coeval calc-alkaline eruptions in the Weeksboro–Lunksoos Lake and Munsungun Cambrian-Ordovician inliers in northeastern Maine are not consistent with tectonic models involving northwestward migration of a single arc, but rather suggest activity of multiple arcs.

Future research

This paper is a report of progress made during nearly half a century of mapping in the Miramichi Cambrian–Ordovician inlier in Maine (Ludman 1978, 1991, 2003, 2020, in press) and recent studies in the Munsungun inlier (Wang 2018, 2019, 2021). Much of that work is ongoing, and future improvements in understanding their stratigraphy and relationships with the cover rocks will undoubtedly require further revisions in regional tectonic models. Increased interest in volcanic-hosted ore deposits at Pickett and Bald mountains in the Weeksboro–Lunksoos Lake and Munsungun inliers has generated useful geochemical and geochronologic data and further development of these prospects will continue to provide valuable new information.

Additional mapping

Recent mapping in the Munsungun (Wang 2019, 2021) and Miramichi terranes in Maine has been aided by a vast network of lumber roads and recreational trails that provide access (and outcrops) in previously remote areas. Although mapping has vastly improved understanding of these inliers, little work has been done in the Weeksboro–Lunksoos Lake belt and more is needed.

The studies cited above reveal that multiple episodes of hitherto unsuspected faulting are responsible for the current relationships between Cambrian–Ordovician and cover rocks, and for juxtaposing strata within each inlier. Connecting those faults is as important as correlating stratified rocks – indeed, it is critical to understanding which of those units *can* be correlated.

Expanded geochronologic and geochemical studies

Improved understanding of Miramichi volcanic stratigraphy requires a strategic approach to sampling for both geochronology and geochemistry. For example, two of the

Ludman et al. – Age, chemistry, and tectonic setting of Miramichi terrane (Early Paleozoic) volcanic rocks, eastern and east-central Maine, USA

Copyright © Atlantic Geology, 2021

three dates reported above for the Olamon Stream Formation in the Greenfield segment come from the upper member, and the third is from a large float block whose lithology is observed in both upper and lower members. Neither geochemical nor geochronologic data are available for the lower member, nor geochronologic data for basalt in the Olamon Stream Formation, and no geochronologic information from the Stetson Mountain Formation in the Danforth segment. These data are needed to confirm correlation with the Greenfield segment and make more precise correlations with the Meductic Group.

The age of the Meductic Group volcanic rocks in New Brunswick is based on a single sample from the basal Porten Road Formation (Mohammadi *et al.* 2019). Additional ages for that formation and from the overlying Eel River and Oak Mountain formations would reveal the duration of volcanism in this segment of the Popelogan arc and clarify correlation with the Miramichi volcanic rocks in Maine.

REFERENCES

Ayuso, R., Wooden, J., Foley, N., Slack, J., Sinha, A., and Persing, H. 2003. Pb isotope geochemistry and U–Pb zircon (SHRIMP–RG) ages of the Bald Mountain and Mount Chase massive sulfide deposits, northern Maine: Mantle and crustal contributions in the Ordovician. Economic Geology Monograph 11, pp. 589–609. https://doi.org/10.5382/Mono.11.26

Chi, G. and Watters, S. 2002. Preliminary geological and petrographic study of the Poplar Mountain Au occurrence, southwestern New Brunswick. Geological Survey of Canada, Current Research 2002-D6, 11 p. https://doi.org/10.4095/213241

Chi, G., Watters, S., Davis, W., Ni, P., Castonguay, S., and Hoy, D. 2008. Geological, Geochemical and Geochronological Constraints on the Genesis of Gold Mineralization at Poplar Mountain, western New Brunswick. Exploration and Mining Geology, 17, pp. 101–130. https://doi.org/10.2113/gsemg.17.1-2.101

Cohen, K., Finney, S., Gibbard, P., and Fan, J.-X. 2013. The ICS International Chronostratigraphic Chart (updated 2021). Episodes 36, pp. 199–204. https://doi.org/10.18814/epiiugs/2013/v36i3/002

Ekren, E. and Frischknecht, F. 1967. Investigations of bedrock in the Island Falls quadrangle, Aroostook and Penobscot counties, Maine. United States Geological Survey Professional Paper 527, 36 p. https://doi.org/10.3133/pp527

Fyffe, L. 2001. Stratigraphy and geochemistry of Ordovician volcanic rocks of the Eel River area, west-central New Brunswick. Atlantic Geology, 37, pp. 81–101. https://doi.org/10.4138/1973

Fyffe, L. 2005. Bedrock geology of the Rollingdam area (NTS 21 G/06), Charlotte County, New Brunswick. New Brunswick Department of Natural Resources, Minerals, Policy and Planning Division. Plate 2005-29, scale 1:50 000.

Fyffe, L., Lutes, G., and St. Peter, C. 2005a. Bedrock geology of the McAdam area (NTS 21 G/11), York County, New Brunswick. New Brunswick Department of Natural Resources, Minerals, Policy and Planning Division. Plate 2005-34, scale 1:50 000.

Fyffe, L., Venugopal, D., and Lutes, G., 2005b. Bedrock geology of the Fosterville area (NTS 21 G/13), York and Carleton counties, New Brunswick. New Brunswick Department of Natural Resources, Minerals, Policy and Planning Division. Plate 2005-36, scale 1:50 000.

Fyffe, L., Johnson, S., and van Staal, C., 2011. A review of Proterozoic to Early Paleozoic lithotectonic terranes in the northeastern Appalachian orogen of New Brunswick, Canada, and their tectonic evolution during Penobscot, Taconic, Salinic, and Acadian orogenesis. Atlantic Geology, 47, pp. 211–248. https://doi.org/10.4138/atlgeol.2011.010

Hall, B. 1970. Stratigraphy of the southern end of the Munsungun anticlinorium, Maine. Maine Geological Survey Bulletin 22, 63 p.

Hall, R. and Nichols, G. 1990. Terrane amalgamation in the Philippine Sea margin. Tectonophysics, 181, pp. 207–222. https://doi.org/10.1016/0040-1951(90)90017-3

Hibbard, J., van Staal., C., Rankin, D., and Williams, H. 2006. Lithotectonic map of the Appalachian orogen, Canada-United States of America. Geological Survey of Canada, Map 2096A, scale 1:1 500 000. https://doi.org/10.4095/221912

Irvine, T. and Baragar, W. 1971. A guide to the chemical

classification of the common volcanic rocks. Canadian Journal of Earth Science, 8, pp. 523–548. https://doi.org/10.1139/e71-055

Kramers, J. and Tolstikhin, I. 1997. Two terrestrial lead isotope paradoxes, forward transport modeling, core formation and the history of the continental crust. Chemical Geology, 139, pp. 75–110. https://doi.org/10.1016/S0009-2541(97)00027-2

Larrabee, D, Spencer, C., and Swift D. 1965. Bedrock geology of the Grand Lake area, Aroostook, Hancock, Penobscot, and Washington Counties, Maine. United States Geological Survey Bulletin 1201, 38 p.

LeBas, M., LeMaitre, R., Streckeisen, A., and Zanettin, B. 1986. A chemical classification of volcanic rocks based on the total alkali-silica diagram. Journal of Petrology, 27, pp. 745–750. https://doi.org/10.1093/petrology/27.3.745

Llamas, A. and Hepburn, J. C. 2013. Geochemistry of Silurian–Devonian volcanic rocks in the Coastal Volcanic belt, Machias–Eastport area, Maine: Evidence for a pre-Acadian arc. Geological Society of America Bulletin, 125, pp. 1930–1942. https://doi.org/10.1130/B30776.1

Ludman, A. 1978, Stratigraphy and structure of Silurian and pre-Silurian rocks in the Brookton–Princeton area, eastern Maine. In Guidebook for trips in southeastern Maine and southwestern New Brunswick. Edited by A. Ludman. New England Intercollegiate Geological Conference pp. 145–161.

Ludman, A. 1985. Pre-Silurian rocks of eastern and southeastern Maine. Maine Geological Survey Open File Report 85-78, 29 p.

Ludman, A. 1991. Stratigraphy of the Miramichi terrane in eastern Maine. In Geology of the Coastal Lithotectonic Belt and neighboring terranes, eastern Maine and southern New Brunswick. Edited by A. Ludman. New England Intercollegiate Geological Conference Guidebook, pp. 338–357.

Ludman, A. 2003. Bedrock Geology of the Dill Hill 7½' quadrangle, Maine. Maine Geological Survey Open File Report OF 03-93, 16 p, scale 1:24 000.

Ludman, A., 2020. Bedrock geology of the Greenfield quadrangle, Maine: Maine Geological Survey, Open-File Report 20-10, 43 p., scale 1:24000.

Ludman, A. in press. Revised bedrock geology of the Greenfield quadrangle, Maine; Maine 1105 Geological Survey, Open File Report, scale 1:24 000.

Ludman, A. and Berry, H. 2003. Bedrock Geologic Map of the Calais 1:100 000 quadrangle; Maine Geological Survey Open File Report, OF 03-97, scale 1:100,000.

Ludman, A., Aleinikoff, J., Berry, H., and Hopeck, J. 2018. SHRIMP U–Pb zircon evidence for age, provenance, and tectonic history of early Paleozoic Ganderian rocks, east-central Maine; Atlantic Geology, 54, pp. 335–387. https://doi.org/10.4138/atlgeol.2018.012

Ludman, A. and Hopeck, J. 2020. Bedrock Geology of the Springfield 15' quadrangle, Maine: Maine Geological Survey, Open-File Report 20-22, 20 p, four 1:24 000 scale geologic maps.

Lutes, G., 2005. Bedrock geology of the Forest City area (NTS 21 G/12), York County, New Brunswick. New Brunswick Department of Natural Resources, Minerals, Policy and Planning Division. Plate 2005-35, scale 1:50 000.

Lutes, G., Venugopal, D., and St. Peter, C., 2005. Bedrock geology of the Canterbury area (NTS 21 G/14), York County, New Brunswick. New Brunswick Department of Natural Resources, Minerals, Policy and Planning Division. Plate 2005-37, scale 1:50 000.

McCormick, M., 2021 (in review). Geology and lithochemistry of the Pickett Mountain volcanogenic massive sulfide deposit, northern Maine. MSc. thesis, University of Maine at Orono.

McClenaghan, S., Lentz, D., and Fyffe, L. 2006. Chemostratigraphy of volcanic rocks hosting massive sulfide clasts within the Meductic Group, west-central New Brunswick. Exploration and Mining Geology, 15, pp. 241–261. https://doi.org/10.2113/gsemg.15.3-4.241

Mohammadi, N., Fyffe, L., McFarlane, C., Wilson, R., and Lentz, D. 2019. U–Pb zircon and monazite geochronology of volcanic and plutonic rocks in southwestern, central, and northeastern New Brunswick. Geological Survey of Canada, Open File 8581, 46 p. https://doi.org/10.4095/314824

Neuman, R. 1967. Bedrock geology of the Shin Pond and Stacyville quadrangles, Penobscot County, Maine. United States Geological Survey Professional Paper 524-I, 37 p. https://doi.org/10.3133/pp524I

Olson, R. 1972. Bedrock geology of the southwest one sixth of the Saponac quadrangle, Penobscot and Hancock counties, Maine; Unpublished M.S. thesis, University of Maine, Orono, Maine, 60 p.

Osberg, P., Hussey, A., and Boone, G. 1985. Bedrock Geologic Map of Maine. Maine Geological Survey, scale 1:500 000.

Paces, J. and Miller, J. 1993. Precise U–Pb Ages of Duluth Complex and Related Mafic Intrusions, Northeastern Minnesota - Geochronological Insights to Physical, Petrogenetic, Paleomagnetic, and Tectonomagmatic Processes Associated with the 1.1 Ga Midcontinent Rift System. Journal of Geophysical Research – Solid Earth, 98, pp. 13997–14013. https://doi.org/10.1029/93JB01159

Pearce, J., Harris, B., and Tindle, A. 1984. Trace element discrimination diagrams for the tectonic interpretation of granitic rocks. Journal of Petrology, 25, pp. 956–983. https://doi.org/10.1093/petrology/25.4.956

Petrus, J. and Kamber, B. 2012. VizualAge: A novel approach to laser ablation ICP-MS U–Pb geochronology data reduction. Geostandards and Geoanalytical Research, 36, pp. 247–270. https://doi.org/10.1111/j.1751-908X.2012.00158.x

Sayres, M. 1986. Stratigraphy, polydeformation, and tectonic setting of Ordovician volcanic rocks in the Danforth area, eastern Maine. Unpublished M.A. thesis, Queens College (City University of New York), Flushing, New York, 135 p.

Slama, J., Kosler, J., Condon, D., Crowley, J., Gerdes, A., Hanchar, J., Horstwood, M., Morris, G., Nasdala, L., Nor-

berg, N., Schaltegger, U., Schoene, B., Tubrett, M., and Whitehouse, M. 2008. Plesovice zircon - A new natural reference material for U–Pb and Hf isotopic microanalysis. Chemical Geology, 249, pp. 1–35. https://doi.org/10.1016/j.chemgeo.2007.11.005

Smith, E. and Fyffe, L. (compilers), 2006a. Bedrock geology of the Millville area (NTS 21 J/03), York and Carleton counties, New Brunswick. New Brunswick Department of Natural Resources, Minerals, Policy and Planning Division. Plate 2006-4, scale 1:50 000.

Smith, E. and Fyffe, L. (compilers), 2006b. Bedrock geology of the Woodstock area (NTS 21 J/04), Carleton County, New Brunswick. New Brunswick Department of Natural Resources, Minerals, Policy and Planning Division. Plate 2006-5, scale 1:50 000.

Sullivan, R. and van Staal., C. 1996. Preliminary chronostratigraphy of the Tetagouche and Fournier groups in northern New Brunswick. In Radiogenic Age and Isotopic Studies: Report 9; Geological Survey of Canada, Current Research I995-F, pp. 43–56. https://doi.org/10.4095/207762

van Staal, C., Wilson, R., Rogers, N., Fyffe, L., Langton, J., McCutcheon, S., McNicoll, V., and Ravenhurst, C., 2003. Bedrock Geology, tectonic setting, and metamorphism. In Massive sulfide deposits of the Bathurst mining camp, New Brunswick and northern Maine. Edited by Goodfellow, W., McCutcheon, S., and Peter, J. Society of Economic Geologists, pp. 37–60.

van Staal, C., Wilson, R., Kamo, S., McClelland, W., and McNicoll, V. 2016. Evolution of the Early to Middle Ordovician Popelogan arc in New Brunswick, Canada and adjacent Maine, USA: Record of arc-trench migration and multiple phases of rifting. Geological Society of America Bulletin, 128, pp. 122–146. https://doi.org/10.1130/B31253.1

Wang, Chunzeng, 2018. Bedrock geology of the Round Mountain quadrangle, Maine. Maine Geological Survey, Open-File Map 18-8, scale 1:24 000.

Wang, Chunzeng, 2019. Bedrock geology of the Jack Mountain quadrangle, Maine. Maine Geological Survey, Open-File Map 19-6, scale 1:24 000.

Wang, Chunzeng, 2021. Bedrock geology of the Big Machias Lake quadrangle, Maine. Maine Geological Survey, Open-File Map 21-12, scale 1:24 000.

Winchester, J., van Staal, C., and Fyffe, L. 1992. Ordovician volcanic and hypabyssal rocks in the central and southern Miramichi Highlands: their tectonic setting and relationship to contemporary volcanic rocks in northern New Brunswick. Atlantic Geology, 28, pp. 171–179. https://doi.org/10.4138/1859

Wood, D., Joron, J-L., and Treuil, M. 1979. A re-appraisal of the use of trace elements to classify and discriminate between magma series erupted in different tectonic settings. Earth and Planetary Science Letters, 45, pp. 326–336. https://doi.org/10.1016/0012-821X(79)90133-X

Editorial responsibility: David P. West, Jr.

Appendix A. Whole-rock analyses for major, trace, and rare earth elements from the Greenfield and Danforth segments.

GREENFIELD SEGMENT (Olamon Stream Formation)																				
Sample	17A58	17A58a	18B30	18B37a	18B37b	18B58	18B59	18B70	18B70b	19A2	19A7	19A8	19A38	19A39	19A53	19A54	19A60	19A61	81G11	13A78
Major elements (wt. %)																				
SiO$_2$	55.56	49.10	67.05	60.19	71.63	46.40	77.00	56.97	58.11	65.85	84.61	78.34	46.73	49.08	46.75	54.68	78.25	78.49	63.10	64.44
Al$_2$O$_3$	15.94	17.51	15.05	15.53	12.06	15.10	10.14	15.55	15.38	14.74	6.68	10.11	18.17	16.47	17.27	15.53	11.59	11.35	16.60	14.91
TiO$_2$	1.22	1.41	0.44	0.64	0.40	0.39	0.23	0.42	0.41	0.67	0.56	0.23	1.31	1.31	1.15	1.11	0.18	0.18	0.53	0.56
Fe$_2$O$_3$^{T}	9.90	10.94	6.37	8.83	4.10	11.54	2.63	9.05	8.44	5.03	4.22	2.33	10.49	10.50	9.72	9.00	2.54	2.32	5.45	4.60
MnO	0.12	0.17	0.23	0.50	0.33	2.47	0.23	0.16	0.19	0.15	0.04	0.45	0.16	0.14	0.17	0.13	0.08	0.10	0.09	0.15
MgO	3.78	5.92	1.74	3.61	1.82	1.75	0.62	5.11	4.52	1.42	0.59	0.52	4.80	5.55	4.61	3.42	0.57	0.65	3.28	1.88
CaO	5.90	5.61	0.63	1.44	2.30	5.99	1.71	5.00	3.61	2.31	0.11	1.58	8.11	8.53	9.98	7.88	0.15	0.17	3.60	1.20
Na$_2$O	4.50	4.22	6.31	4.40	1.29	3.63	1.55	5.46	5.88	2.68	0.85	3.36	3.33	3.12	3.12	3.54	2.02	0.75	2.05	7.15
K$_2$0	0.35	0.96	0.81	1.09	2.98	2.44	2.96	0.55	0.61	2.68	1.08	1.36	0.57	1.54	1.09	0.14	3.02	3.87	1.83	0.34
P$_2$O$_5$	0.23	0.28	0.09	0.11	0.06	0.18	0.05	0.07	0.07	0.16	0.08	0.05	0.22	0.27	0.20	0.14	0.03	0.03	0.17	0.15
LOI	3.35	4.09	2.05	3.67	3.43	8.53	2.76	2.41	2.42	3.43	1.44	2.25	5.28	3.22	6.45	4.74	1.85	2.06	2.93	2.95
Total	100.90	100.20	100.80	100.00	100.40	98.52	99.98	100.80	99.62	100.50	100.30	100.60	99.20	99.80	100.50	100.30	100.30	100.00	100.30	98.30
Selected trace elements (ppm)																				
Ba	127	271	481	495	868	4593	1323	301	410	2993	178	567	189	168	396	92	1564	2014		
Cr	130	90	30	20	< 20	60	< 20	140	110	< 20	40	< 20	30	110	40	30	< 20	< 20		
Cu	70	100	40	70	20	110	10	120	100	10	10	< 10	100	40	70	70	< 10	< 10		
Ga	20	20	16	19	14	19	11	17	17	18	9	10	20	19	21	18	14	13		
Nb	5	6	4	3	4	5	6	2	3	10	8	6	6	6	5	4	5	5		
Ni	30	40	< 20	< 20	< 20	60	< 20	50	40	< 20	< 20	< 20	< 20	40	30	30	< 20	< 20		
Rb	6	17	15	31	92	80	108	8	10	90	48	46	12	28	24	2	96	120		
Sr	142	251	94	166	86	380	111	132	137	219	28	170	328	422	231	163	100	53		
V	332	295	117	172	32	147	12	267	235	61	45	11	296	233	255	272	5 <	5 <		
Y	20	31	19	17	28	19	32	8	11	25	20	27	25	27	23	19	34	32		
Zn	70	120	70	110	80	100	30	70	80	70	40	30 <	100	130	90	90	40	50		
Zr	109	130	89	62	107	84	160	58	62	210	346	145	108	144	100	83	155	153		
Rare Earth elements (ppm)																				
La	13.7	16.1	13.9	9.00	12.7	20.8	23.3	6.9	7.9	29.1	26.5	22.1	12.6	14.9	12.8	10.4	15.3	15.9		
Ce	29.1	36.0	29.0	20.20	27.5	51.5	49.3	15.0	17.2	60.1	57.7	47.6	29.3	33.9	29.0	23.7	32.5	33.4		
Pr	3.64	4.6	3.29	2.49	3.34	4.52	5.53	1.79	1.99	6.84	6.24	5.21	3.81	4.3	3.75	3.1	3.7	3.9		
Nd	15.8	20.6	13.1	10.9	14.4	18.4	21.9	7.4	8.1	27.0	23.9	20.4	17.2	19.0	16.7	13.7	15.5	16.2		
Sm	3.8	5.1	3.1	2.7	3.6	4.1	4.9	1.6	1.8	5.6	4.6	4.6	4.3	4.8	4.2	3.5	3.8	3.9		
Eu	1.15	1.7	0.8	0.94	0.93	1.02	0.80	0.49	0.53	1.34	0.98	0.74	1.37	1.5	1.36	1.12	0.67	0.67		
Gd	3.9	5.8	3.0	3.1	4.2	3.9	5.0	1.6	2.0	4.8	3.9	4.5	4.6	5.6	4.3	3.8	4.2	4.3		
Tb	0.6	0.9	0.5	0.5	0.8	0.6	0.9	0.3	0.3	0.7	0.6	0.8	0.7	0.9	0.7	0.6	0.7	0.8		
Dy	3.8	5.9	3.2	3.3	4.9	3.8	5.3	1.6	2.0	4.3	3.7	4.8	4.8	5.3	4.4	3.8	4.9	4.8		
Ho	0.8	1.2	0.7	0.7	1.1	0.8	1.1	0.3	0.4	0.8	0.7	1.0	1.0	1.1	0.9	0.7	1.0	1.1		
Er	2.3	3.7	2.2	2.2	3.3	2.3	3.3	1.0	1.3	2.5	2.2	3.1	2.9	3.0	2.7	2.2	3.3	3.3		
Tm	0.34	0.6	0.3	0.33	0.52	0.34	0.50	0.16	0.19	0.38	0.33	0.47	0.42	0.45	0.40	0.34	0.53	0.51		
Yb	2.3	3.6	2.3	2.2	3.5	2.3	3.30	1.0	1.3	2.5	2.3	3.2	2.8	3.0	2.6	2.3	3.7	3.5		
Lu	0.37	0.6	0.4	0.37	0.56	0.34	0.52	0.17	0.21	0.39	0.35	0.49	0.42	0.45	0.40	0.34	0.56	0.57		

Appendix A. Continued.

	OVM	14B17	14B19a	14B19b	83A3b	83A36	83B12a	83B16	83B20	CHERTY	MS211	MS218	MS225	MS242	MS249	MS224b	OWL	78A23

DANFORTH SEGMENT (Stetson Mountain Formation)

Major elements (wt. %) (numbers in italic are from Sayres 1986)

	OVM	14B17	14B19a	14B19b	83A3b	83A36	83B12a	83B16	83B20	CHERTY	MS211	MS218	MS225	MS242	MS249	MS224b	OWL	78A23
SiO_2	54.20	62.82	62.54	65.96	*71.00*	*62.10*	*77.00*	*64.50*	*73.30*	*76.40*	*62.20*	*68.60*	*76.60*	*74.60*	*73.20*	*70.10*	*70.30*	*52.80*
Al_2O_3	19.59	14.72	14.56	14.05	*13.50*	*16.20*	*11.60*	*15.80*	*14.40*	*11.80*	*14.00*	*14.00*	*11.60*	*12.30*	*11.10*	*13.60*	*14.90*	*18.20*
TiO_2	1.17	0.48	0.53	0.45	*0.36*	*0.65*	*0.23*	*0.58*	*0.36*	*0.19*	*0.73*	*0.46*	*0.32*	*0.35*	*0.20*	*0.41*	*0.53*	*1.35*
$Fe_2O_3^T$	7.05	6.90	6.78	6.77	*4.98*	*6.42*	*1.55*	*5.31*	*2.73*	*1.87*	*7.36*	*4.49*	*1.66*	*3.73*	*1.68*	*3.12*	*4.26*	*10.10*
MnO	0.18	0.23	0.22	0.17	*0.07*	*0.09*	*0.09*	*0.07*	*0.05*	*0.07*	*0.19*	*0.22*	*0.08*	*0.04*	*0.13*	*0.15*	*0.12*	*0.12*
MgO	2.72	3.24	2.91	2.99	*1.01*	*2.31*	*0.66*	*1.80*	*0.88*	*0.67*	*3.70*	*1.72*	*0.46*	*0.85*	*0.51*	*0.74*	*1.11*	*4.21*
CaO	1.46	3.27	3.86	1.99	*0.57*	*1.42*	*1.40*	*1.49*	*0.17*	*0.47*	*2.33*	*0.84*	*1.60*	*0.07*	*3.85*	*2.44*	*0.76*	*5.03*
Na_2O	1.05	4.23	2.64	3.07	*2.93*	*2.51*	*1.46*	*3.75*	*2.80*	*5.60*	*2.50*	*2.25*	*3.25*	*3.78*	*1.70*	*3.13*	*1.49*	*4.65*
K_2O	4.84	1.13	2.12	3.45	*3.00*	*3.87*	*3.08*	*3.08*	*2.85*	*1.18*	*2.20*	*4.95*	*1.77*	*2.44*	*2.55*	*2.11*	*3.78*	*0.83*
P_2O_5	0.13	0.11	0.14	0.14	*0.10*	*0.13*	*0.04*	*0.12*	*0.07*	*0.04*	*0.25*	*0.15*	*0.05*	*0.07*	*0.04*	*0.07*	*3.13*	*0.25*
LOI	6.54	1.10	2.01	1.56	*2.31*	*3.62*	*2.85*	*3.16*	*2.16*	*1.77*	*4.39*	*1.93*	*2.47*	*1.77*	*5.08*	*3.93*	*2.62*	*2.70*
Total	98.93	98.53	100.60	100.60	*100.30*	*100.00*	*100.20*	*100.40*	*100.10*	*100.30*	*100.20*	*100.00*	*100.10*	*100.30*	*100.30*	*100.10*	*100.20*	*100.40*
	Rare Earth elements (ppm)																	
La	47.1	9.3	15.4	15.9														
Ce	95.3	20.5	33.5	31.3														
Pr	11.6	2.49	4.32	3.91														
Nd	45.7	17.8	15.8	10.4														
Sm	9.2	4.3	3.5	2.5														
Eu	1.54	0.91	0.8	0.74														
Gd	8	4.3	2.8	2.8														
Tb	1.3	0.7	0.5	0.5														
Dy	7.5	5.2	3.3	3.1														
Ho	1.5	1	0.7	0.7														
Er	4.4	3	2.2	2.1														
Tm	0.65	0.46	0.33	0.31														
Yb	4.2	2.8	2.2	2.1														
Lu	0.65	0.41	0.33	0.33														

Major elements for the first four samples (OVM, 14B17, 14B19a, and 14B19B) were analyzed by ICPOES; the rest by XRF (in italic).

LUDMAN ET AL. – Age, chemistry, and tectonic setting of Miramichi terrane (Early Paleozoic) volcanic rocks, eastern and east-central Maine, USA

Copyright © Atlantic Geology, 2021

Appendix B. UTM locations for geochemical and U-Pb samples. U-Pb sample locations are shown in red.

Sample	Quadrangle	UTM83X	UTM83Y
14B17	Bottle Lake	573935	5024722
14B19a	Bowers Mtn	573842	5025082
14B19b	Bowers Mtn	573842	5025082
OVM	Farrow Mountain	593303	5026707
13A78	**Greenfield**	**545178**	**4984202**
18B30	Greenfield	539545	4985063
18B37a	Greenfield	539799	4985822
18B37b	Greenfield	539799	4985822
18B58	Greenfield	543307	4990403
18B59	Greenfield	542474	4990309
18B70	**Greenfield**	**542232**	**4990556**
18B70b	Greenfield	542232	4990556
19A2	Greenfield	541477	4987832
19A7	Greenfield	541045	4988245
19A8	Greenfield	543307	4990403
19A60	Greenfield	542266	4989257
19A61	**Greenfield**	**542338**	**4989153**
19A38	Olamon	538683	4983353
19A39	Olamon	538750	4983296
19A53	Olamon	538552	4983326
19A54	Olamon	538515	4983302
17A58	Otter Chain Ponds	537797	4982716
17A58a	Otter Chain Ponds	537797	4982716

All data are in NAD83, UTM zone 19N (m)

Appendix C. Laser ablation (LA-ICP-MS) analyses of zircons from Greenfield segment rocks.

Spot	Concentrations			common-Pb				Final isotope ratios							Final ages (Ma)						
	U (ppm)	Th (ppm)	U/Th	204Pb cps	2σ int	206Pb/204Pb	%Pb*	207Pb/235U	2σ	206Pb/238U	2σ	err. corr.	207Pb/206Pb	2σ	207Pb/206Pb	2σ	207Pb/235U	2σ	206Pb/238U	2σ	% conc
Andesitic crystal tuff (sample 20A13)																					
20A13 - 10*	146.4	63.1	2.32	-11	13	5380	100.16	0.55	0.03	0.076	0.001	0.057	0.052	0.003	284	98	442	17	470.7	9	106.5
20A13 - 9*	198	110.8	1.79	-19	14	7270	99.95	0.57	0.02	0.076	0.001	0.191	0.055	0.002	372	87	455	16	473.6	8	104.1
20A13 - 3	94.9	47.1	2.01	2	11	1810	99.97	0.60	0.03	0.078	0.002	0.062	0.055	0.003	380	110	470	21	485.7	10	103.3
20A13 - 11*	137.1	68.6	2.00	0	14	4950	100.00	0.57	0.03	0.075	0.002	0.098	0.054	0.003	390	120	457	21	467.9	9	102.4
20A13 - 26	111.7	49.4	2.26	12	14	363	99.91	0.61	0.03	0.079	0.002	0.067	0.057	0.003	430	120	486	21	488.8	10	100.6
20A13 - 2*	78.4	27.5	2.85	3	10	1020	99.83	0.60	0.04	0.077	0.002	0.280	0.057	0.004	440	130	474	24	476.3	10	100.5
20A13 - 6*	147.6	59.6	2.48	13	16	374	99.51	0.57	0.03	0.074	0.002	0.137	0.056	0.003	470	120	456	19	457.7	11	100.4
20A13 - 24*	101	54.3	1.86	12	12	333	99.69	0.60	0.03	0.077	0.002	0.021	0.058	0.003	470	120	482	20	479.8	11	99.5
20A13 - 22[3]	2119	544	3.90	650	45	124	84.81	0.54	0.06	0.068	0.001	0.827	0.056	0.006	940	130	425	46	422.7	7	99.5
20A13 - 17*	157.2	89.9	1.75	-3	14	5800	99.63	0.60	0.03	0.077	0.001	0.050	0.058	0.003	498	96	481	17	475.7	8	98.9
20A13 - 20*	150.4	69.3	2.17	-1	14	5350	99.73	0.59	0.03	0.075	0.002	0.117	0.057	0.003	468	96	473	18	466.7	9	98.7
20A13 - 15	171.7	125.4	1.37	9	13	664	99.74	0.58	0.03	0.073	0.001	0.042	0.057	0.003	500	100	460	18	453.7	8	98.6
20A13 - 5*	165.9	79	2.10	11	12	543	99.53	0.60	0.02	0.075	0.001	0.040	0.059	0.003	552	91	475	15	467.9	8	98.5
20A13 - 25	140.1	70.14	2.00	5	12	5142	99.35	6.72	0.11	0.374	0.006	0.131	0.130	0.002	2095	24	2074	15	2049.0	26	97.8
20A13 - 16*	151.7	135.4	1.12	0	14	5700	99.38	0.61	0.02	0.076	0.001	0.054	0.059	0.002	528	85	483	15	469.8	8	97.3
20A13 - 21	1075	274.3	3.92	13	23	2238	99.34	0.53	0.02	0.065	0.001	0.194	0.058	0.002	517	69	430	12	404.1	7	94.0
20A13 - 18	234.1	202.5	1.16	13	14	3253	98.98	6.26	0.10	0.353	0.005	0.253	0.129	0.002	2075	23	2012	14	1948.0	24	93.2
20A13 - 19	71.2	36.4	1.96	8	13	327	99.31	0.65	0.04	0.077	0.002	0.006	0.061	0.004	610	130	511	25	475.5	11	93.1
20A13 - 8	50.58	34.5	1.47	-10	12	1772	99.07	0.64	0.04	0.074	0.002	0.033	0.063	0.004	650	140	500	25	459.6	10	91.9
20A13 - 7	220.3	129.2	1.71	-12	17	7100	99.16	0.61	0.03	0.071	0.002	0.348	0.061	0.003	630	110	483	21	442.0	9	91.5
20A13 - 13	144.5	78.1	1.85	17	18	347	98.73	0.71	0.04	0.078	0.002	0.051	0.068	0.004	790	130	545	24	484.0	11	88.8
20A13 - 1	177.2	84.9	2.09	-4	15	6480	98.22	0.72	0.03	0.075	0.002	0.198	0.070	0.003	892	95	555	20	468.6	9	84.4
20A13 - 12[3]	228.8	176.7	1.29	534	30	35	55.12	1.50	0.44	0.093	0.004	0.895	0.108	0.031	2770	150	940	180	571.0	24	60.7
Microporphyritic rhyolitic tuff (sample 20A15)																					
20A15 - 20	585	223	2.62	69	16	547	97.11	0.87	0.13	0.107	0.002	0.683	0.057	0.007	1070	150	592	73	656.9	12	111.0
20A15 - 32	308.3	108.1	2.85	5	12	6603	99.76	2.30	0.04	0.209	0.004	0.187	0.079	0.001	1167	30	1209	14	1221.0	20	106.5
20A15 - 16	63.03	56.3	1.12	-6	12	3202	99.93	0.80	0.04	0.103	0.002	0.027	0.057	0.003	480	110	596	22	629.0	14	105.5
20A15 - 22	33.19	18.53	1.79	-6	13	5898	99.12	5.70	0.20	0.353	0.008	0.347	0.117	0.004	1897	57	1938	31	1951.0	40	104.1
20A15 - 24	47.12	43.93	1.07	2	12	1137	100.15	0.75	0.05	0.096	0.002	0.018	0.056	0.004	420	140	572	30	588.0	14	102.8
20A15 - 14	41.5	29.2	1.42	11	13	256	99.44	1.19	0.07	0.134	0.003	0.015	0.065	0.004	760	120	797	31	808.0	18	101.4
20A15 - 1	221	104	2.13	-7	12	10660	99.59	0.80	0.03	0.098	0.002	0.245	0.059	0.002	535	66	598	15	603.5	10	100.9
20A15 - 31*	188.7	117	1.61	8	13	910	99.83	0.58	0.03	0.075	0.001	0.077	0.056	0.003	422	99	460	17	464.2	8	100.9

Appendix C. Continued.

Spot	Concentrations			common-Pb				Final isotope ratios							Final ages (Ma)						
	U (ppm)	Th (ppm)	U/Th	204Pb cps	2σ int	206Pb/204Pb	%Pb*	207Pb/235U	2σ	206Pb/238U	2σ	err. corr.	207Pb/206Pb	2σ	207Pb/206Pb	2σ	207Pb/235U	2σ	206Pb/238U	2σ	% conc
20A15 - 9	268.2	182.3	1.47	-5	19	42944	99.80	4.28	0.09	0.303	0.005	0.388	0.103	0.002	1682	29	1691	17	1704.0	24	100.9
20A15 - 23	131.1	124.9	1.05	5	12	1388	99.55	0.88	0.04	0.104	0.002	0.046	0.060	0.003	595	93	635	21	640.0	10	100.8
20A15 - 8	259	51.8	5.00	-3	14	15030	99.65	0.97	0.03	0.113	0.002	0.191	0.062	0.002	666	52	686	13	689.7	10	100.5
20A15 - 29	241.9	276.6	0.87	16	13	777	99.65	0.82	0.02	0.100	0.002	0.206	0.060	0.002	575	59	609	13	612.1	9	100.5
20A15 - 11*	154.8	91	1.70	15	14	389	99.70	0.59	0.03	0.076	0.001	0.107	0.057	0.003	448	93	473	17	474	8	100.1
20A15 - 10	244	164.9	1.48	-8	13	11080	99.52	0.73	0.02	0.090	0.002	0.081	0.059	0.002	535	65	557	14	557	9	99.9
20A15 - 2	378	487	0.78	-12	19	19538	99.66	0.79	0.03	0.096	0.002	0.327	0.059	0.002	586	76	589	14	589	11	99.9
20A15 - 17	165.7	83.1	1.99	-3	16	16020	99.46	2.15	0.06	0.194	0.004	0.374	0.079	0.002	1161	50	1162	21	1145	19	99.3
20A15 - 28	296.6	161.2	1.84	13	12	3475	99.75	4.22	0.07	0.295	0.004	0.252	0.103	0.001	1670	24	1677	13	1671	22	99.2
20A15 - 5	241.3	116.2	2.08	6	12	2047	99.54	0.82	0.02	0.098	0.002	0.036	0.060	0.002	594	64	610	13	603	10	98.9
20A15 - 33	316.5	171.7	1.84	-3	14	15300	99.53	0.92	0.03	0.106	0.002	0.102	0.062	0.002	672	58	660	13	651	10	98.7
20A15 - 36	163.7	52.9	3.09	25	17	791	99.29	2.92	0.07	0.234	0.004	0.283	0.089	0.002	1398	44	1385	19	1354	21	98.6
20A15 - 25	395	229.5	1.72	-9	17	16320	99.57	0.59	0.02	0.075	0.001	0.201	0.057	0.002	510	60	470	11	464	7	98.6
20A15 - 37	315.3	398	0.79	16	12	868	99.51	0.68	0.02	0.084	0.002	0.196	0.059	0.002	540	61	530	12	522	9	98.4
20A15 - 30	258.7	47.56	5.44	3	13	5653	99.52	1.19	0.03	0.129	0.002	0.049	0.066	0.002	793	51	795	14	781	12	98.2
20A15 - 12	85.2	53.96	1.58	-10	14	9810	99.57	2.37	0.09	0.209	0.004	0.285	0.082	0.003	1256	74	1228	29	1222	21	96.7
20A15 - 18	454.5	263.6	1.72	-3	17	59595	99.41	3.47	0.05	0.257	0.004	0.203	0.096	0.001	1546	22	1519	12	1474	19	96.7
20A15 - 27	500	218	2.29	6	12	4667	99.53	0.93	0.02	0.105	0.002	0.331	0.063	0.001	706	41	668	11	641	10	95.9
20A15 - 13	486	221	2.20	17	14	1455	99.30	0.92	0.02	0.102	0.002	0.260	0.066	0.001	797	40	665	11	624	9	93.9
20A15 - 21	129.7	108.1	1.20	3	13	2930	99.01	1.35	0.05	0.134	0.003	0.293	0.072	0.002	1011	62	870	19	809	14	93.0
20A15 - 19	203.6	186	1.09	25	16	1423	98.96	5.37	0.09	0.324	0.006	0.733	0.119	0.002	1943	23	1881	14	1810	27	92.9
20A15 - 6	252.6	65.9	3.83	1	16	24400	99.19	2.29	0.05	0.196	0.003	0.102	0.083	0.002	1273	41	1207	17	1151	17	91.4
20A15 - 15	30.95	67.7	0.46	12	16	132	98.14	0.96	0.09	0.099	0.003	0.294	0.074	0.006	920	190	691	47	607	19	87.8
20A15 - 34	129.9	61.3	2.12	9	15	484	98.43	0.67	0.04	0.071	0.002	0.035	0.066	0.004	760	110	513	21	443	10	86.3
20A15 - 3	219.9	483	0.46	24	24	359	98.40	0.87	0.06	0.089	0.002	0.231	0.069	0.004	910	120	641	29	550	11	85.7
20A15 - 35	221.7	148.2	1.50	14	15	644	97.85	0.72	0.04	0.071	0.001	0.370	0.072	0.004	980	110	550	24	445	8	80.9
20A15 - 7	104	49.9	2.08	-3	16	3800	97.49	0.82	0.05	0.078	0.002	0.205	0.075	0.005	1000	130	605	28	486	11	80.3
20A15 - 26	32.5	36	0.90	15	11	101	94.84	1.29	0.11	0.093	0.003	0.383	0.101	0.009	1550	160	835	50	574	16	68.7
20A15 - 4	157.4	88.8	1.77	31	19	194	90.70	1.44	0.09	0.079	0.002	0.260	0.129	0.008	2030	120	900	41	490	12	54.5

Appendix C. Continued.

Spot	Concentrations			common-Pb				Final isotope ratios							Final ages (Ma)						
	U (ppm)	Th (ppm)	U/ Th	^{204}Pb cps	2σ int	^{206}Pb/ ^{204}Pb	%Pb*	^{207}Pb/ ^{235}U	2σ	^{206}Pb/ ^{238}U	2σ	err. corr.	^{207}Pb/ ^{206}Pb	2σ	^{207}Pb/ ^{206}Pb	2σ	^{207}Pb/ ^{235}U	2σ	^{206}Pb/ ^{238}U	2σ	% conc
Basalt (sample 20A8)																					
20A8 - 16	217	101	2.15	-1	18	31974	99.47	3.32	0.08	0.260	0.005	0.179	0.096	0.003	1553	62	1486	19	1487	27	108.1
20A8 - 23[3]	2728	1245	2.19	1030	110	118	85.60	0.45	0.09	0.066	0.002	0.647	0.055	0.009	910	220	382	61	409	9	107.1
20A8 - 3	171.2	59.7	2.87	8	12	1686	99.50	2.11	0.07	0.196	0.002	0.106	0.078	0.002	1143	60	1153	22	1156	12	101.5
20A8 - 21	260	108.3	2.40	21	15	635	99.61	0.76	0.03	0.093	0.002	0.396	0.059	0.002	574	67	572	17	572	12	100.0
20A8 - 6	116.7	68.9	1.69	-2	16	19239	99.57	6.99	0.18	0.387	0.005	0.128	0.131	0.003	2109	39	2111	23	2109	23	99.9
20A8 - 1	311	71.2	4.37	3	16	12371	99.51	3.34	0.07	0.255	0.005	0.255	0.093	0.002	1492	39	1491	18	1462	23	99.7
r2_20A8 - 13	751	43.9	17.11	15	15	6224	99.54	5.27	0.10	0.335	0.003	0.262	0.114	0.002	1860	29	1864	16	1862	16	99.6
r2_20A8 - 9	430.1	114.5	3.76	6	17	3563	99.66	1.04	0.03	0.118	0.001	0.093	0.064	0.002	721	55	724	15	720	8	99.4
20A8 - 31	177.9	80.5	2.21	0	12	21160	99.53	2.76	0.06	0.231	0.004	0.267	0.086	0.002	1340	39	1343	17	1339	20	99.4
r2_20A8 - 10	75.5	77	0.98	1	15	2820	99.66	0.74	0.05	0.090	0.002	0.158	0.060	0.004	540	140	562	33	557	11	99.1
20A8 - 29	644	93.4	6.90	4	12	8103	99.67	0.82	0.02	0.098	0.002	0.103	0.061	0.001	616	40	610	10	604	9	98.9
20A8 - 9	519	317.5	1.63	1	12	24005	99.59	0.72	0.02	0.088	0.001	0.003	0.059	0.002	581	55	550	11	544	8	98.9
20A8 - 24	461	278	1.66	8	11	3619	99.64	1.14	0.02	0.125	0.002	0.136	0.066	0.001	809	38	772	11	761	11	98.7
r2_20A8 - 12	171.6	64.79	2.65	-4	12	18310	99.48	3.58	0.09	0.270	0.003	0.231	0.096	0.002	1557	39	1542	20	1540	16	98.5
20A8 - 19	195.8	122.4	1.60	0	15	34213	99.64	5.52	0.10	0.342	0.005	0.333	0.118	0.002	1917	24	1902	16	1896	24	98.5
20A8 - 7	213	99.7	2.14	8	12	1271	99.46	0.84	0.03	0.099	0.002	0.061	0.062	0.002	665	66	617	15	607	10	98.3
20A8 - 28	247.1	163	1.52	11	14	891	99.40	0.60	0.02	0.075	0.001	0.133	0.058	0.002	536	77	475	13	467	8	98.2
20A8 - 20	341.7	257	1.33	15	11	1189	99.51	0.86	0.02	0.100	0.002	0.060	0.062	0.002	673	50	628	12	616	9	98.2
20A8 - 30	266.7	99.5	2.68	-1	12	16640	99.58	1.10	0.03	0.121	0.002	0.269	0.066	0.001	792	44	753	13	738	11	98.0
r2_20A8 - 14	844	457	1.85	12	18	2950	99.54	0.77	0.03	0.092	0.002	0.062	0.061	0.002	641	81	579	17	568	9	98.0
r2_20A8 - 7	50.8	34.9	1.46	2	12	1307	99.34	1.21	0.07	0.130	0.003	0.050	0.067	0.004	800	120	805	29	789	18	98.0
20A8 - 8	676.1	167.7	4.03	18	20	7972	100.00	11.22	0.16	0.483	0.007	0.629	0.166	0.001	2520	13	2541	14	2540	31	97.7
r2_20A8 - 4	662	540	1.23	0	12	20500	99.56	0.59	0.02	0.074	0.001	0.246	0.058	0.001	511	57	472	11	459	5	97.4
20A8 - 15	507.4	351.4	1.44	0	10	30670	99.58	1.06	0.02	0.117	0.002	0.095	0.066	0.001	797	36	733	10	713	10	97.2
20A8 - 11	271.8	128.8	2.11	6	12	6401	99.75	3.53	0.06	0.267	0.004	0.257	0.096	0.001	1556	26	1533	14	1527	20	97.2
20A8 - 35	397.2	338	1.18	8	13	3398	99.51	1.26	0.03	0.133	0.002	0.259	0.069	0.001	889	36	829	12	804	11	96.9
20A8 - 3	69.9	21.3	3.28	-24	14	6320	99.14	1.82	0.08	0.173	0.003	0.134	0.075	0.003	1074	81	1050	29	1029	18	96.9
20A8 - 33	1504	1370	1.10	19	13	3723	99.59	0.76	0.01	0.089	0.001	0.340	0.062	0.001	668	34	572	8	547	7	95.6
20A8 - 18	91.4	82	1.11	-14	12	5330	98.89	1.07	0.05	0.114	0.002	0.335	0.068	0.003	837	94	734	23	700	14	95.4
20A8 - 2	278.6	79.6	3.50	-18	13	37750	99.52	3.56	0.06	0.267	0.004	0.129	0.098	0.002	1581	29	1540	14	1525	21	95.0
20A8 - 27[2]	2502	1356	1.85	1220	310	79	79.40	0.56	0.08	0.067	0.001	0.708	0.062	0.008	1110	170	439	48	416	7	94.9

Appendix C. Continued.

Spot	Concentrations			common-Pb				Final isotope ratios							Final ages (Ma)						
	U (ppm)	Th (ppm)	U/Th	^{204}Pb cps	2σ int	^{206}Pb/^{204}Pb	%Pb*	^{207}Pb/^{235}U	2σ	^{206}Pb/^{238}U	2σ	err. corr.	^{207}Pb/^{206}Pb	2σ	^{207}Pb/^{206}Pb	2σ	^{207}Pb/^{235}U	2σ	^{206}Pb/^{238}U	2σ	% conc
20A8 - 22	95.4	136.3	0.70	-3	17	16929	99.13	4.97	0.15	0.324	0.008	0.150	0.114	0.003	1862	54	1818	24	1809	39	94.5
r2_20A8 - 5	166.7	85.5	1.95	-1	11	14680	99.23	2.65	0.07	0.219	0.002	0.042	0.087	0.002	1357	48	1311	21	1276	13	94.5
20A8 - 34	841	469	1.79	18	15	2008	99.37	0.68	0.02	0.080	0.001	0.152	0.062	0.001	652	47	529	9	499	7	94.3
20A8 - 6	83.1	45.9	1.81	-8	12	15130	99.02	5.81	0.13	0.344	0.006	0.148	0.123	0.003	2006	38	1953	20	1906	28	93.5
r2_20A8 - 17	880	67.8	12.98	16	17	1562	98.59	0.81	0.04	0.091	0.004	0.617	0.067	0.002	852	65	600	22	559	22	93.2
20A8 - 10	95.1	28	3.40	-9	11	21387	98.12	12.04	0.21	0.475	0.008	0.529	0.183	0.002	2684	22	2607	16	2506	35	92.2
20A8 - 12	260	73.9	3.52	2	11	12553	99.37	2.13	0.05	0.192	0.004	0.443	0.081	0.002	1220	36	1160	16	1129	20	91.7
r2_20A8 - 11	168.4	63.9	2.64	18	22	1171	98.99	3.89	0.12	0.269	0.005	0.095	0.104	0.003	1688	56	1609	25	1535	23	91.0
20A8 - 5	279	99	2.82	4	12	3894	98.82	1.02	0.03	0.104	0.002	0.338	0.070	0.002	943	58	711	14	637	10	89.6
20A8 - 14	402.7	165	2.44	16	13	2642	99.24	2.45	0.04	0.207	0.003	0.203	0.087	0.001	1352	27	1259	13	1211	17	88.0
20A8 - 25	438.7	129.8	3.38	-13	13	59090	99.36	2.87	0.08	0.230	0.005	0.634	0.092	0.002	1484	36	1373	20	1331	24	86.7
20A8 - 26	754	449	1.68	-4	20	25310	98.64	0.52	0.02	0.059	0.002	0.289	0.066	0.002	798	64	428	10	368	11	86.0
r2_20A8 - 8	734	55.4	13.25	20	18	3549	98.67	3.97	0.10	0.268	0.004	0.621	0.108	0.002	1757	30	1627	20	1532	19	85.5
20A8 - 13	676	166	4.07	44	12	638	98.45	0.68	0.02	0.072	0.001	0.088	0.068	0.002	876	55	528	11	450	7	85.3
20A8 - 17³	718	310	2.32	120	22	1343	95.51	10.00	0.27	0.418	0.008	0.745	0.175	0.002	2601	24	2435	26	2253	37	83.6
20A8 - 4	216	74.1	2.91	5	17	3478	96.20	1.89	0.09	0.138	0.006	0.532	0.102	0.005	1657	86	1087	27	830	35	76.4
r2_20A8 - 2	139	42.1	3.30	16	12	658	98.48	2.13	0.08	0.180	0.003	0.352	0.087	0.003	1362	63	1159	24	1067	16	75.2
20A8 - 32	478	14.27	33.50	2	10	51860	91.31	13.03	0.20	0.429	0.007	0.854	0.219	0.001	2973	9	2680	15	2302	33	73.7
r2_20A8 - 1	786	192.4	4.09	48	18	484	96.46	0.81	0.05	0.069	0.001	0.014	0.084	0.005	1290	110	595	26	431	6	72.4
r2_20A8 - 16	497	359	1.38	32	16	463	96.62	0.75	0.04	0.066	0.001	0.722	0.082	0.003	1268	69	570	22	410	9	71.9
r2_20A8 - 15	325	310.4	1.05	34	16	261	88.19	2.20	0.08	0.104	0.002	0.080	0.156	0.006	2405	62	1182	24	639	13	54.1